

Cite this: *J. Mater. Chem. A*, 2024, **12**, 31685

## A holistic review on the direct recycling of lithium-ion batteries from electrolytes to electrodes

Neil Hayagan, <sup>abde</sup> Cyril Aymonier, <sup>ade</sup> Laurence Croguennec, <sup>ade</sup> Mathieu Morcrette, <sup>bde</sup> Rémi Dedryvère, <sup>cde</sup> Jacob Olchowka <sup>\*ade</sup> and Gilles Philippot <sup>\*ade</sup>

Lithium-ion batteries (LIBs) present a global challenge in managing their end-of-life (EOL) issues. As LIB's raw materials are critical and valuable, they are considered as a secondary resource. The volume of publications and patents on LIB recycling has significantly increased, rising a 32% annual growth, compared to a 4% increase in all scientific chemical literature within a decade, reflecting the emergence of this research topic. In a circular economy context, achieving high recycling efficiency of all LIB components and reusing recycled raw materials for battery production are essential. The increase in recycling efficiency is further promoted by government regulations aiming for carbon neutrality and sustainable society with lower environmental impacts. Conventional and destructive recycling methods, pyrometallurgy and hydrometallurgy, focusing on specific metals are insufficient to achieve these goals. Therefore, this review discusses the emerging topic of direct recycling, which recovers, regenerates, and reuses main battery components: electrolyte as well as negative and positive electrodes to fabricate new LIBs. Although this approach may complicate the process, it significantly increases recovery rates, prevents component destruction, and minimizes losses. This critical review offers ideas and methods to provide new perspectives on recycling the main components of LIBs.

Received 18th July 2024  
Accepted 8th October 2024

DOI: 10.1039/d4ta04976d  
[rsc.li/materials-a](http://rsc.li/materials-a)

<sup>a</sup>Univ. Bordeaux, CNRS, Bordeaux INP, ICMCB, UMR 5026, F-33600 Pessac, France.  
E-mail: [jacob.olchowka@icmcb.cnrs.fr](mailto:jacob.olchowka@icmcb.cnrs.fr); [gilles.philippot@icmcb.cnrs.fr](mailto:gilles.philippot@icmcb.cnrs.fr)

<sup>b</sup>Laboratoire de Réactivité et Chimie des Solides, CNRS UMR7314, Université de Picardie Jules Verne, Hub de l'énergie, 15 rue Baudelocque, 80000 Amiens, France  
<sup>c</sup>IPREM, CNRS, Univ. Pau & Pays Adour, E2S UPPA, 64000, Pau, France

<sup>d</sup>Réseau sur le Stockage Electrochimique de l'Energie (RS2E), Hub de l'Energie, CNRS FR 3459, Amiens, France

<sup>e</sup>ALISTORE-ERI European Research Institute, CNRS FR 3104, 80039 Amiens Cedex 1, France



Neil Hayagan

Erasmus Master's program EMerald in 2020. His research interests include conventional and direct recycling of Li-ion batteries.

Neil Hayagan is a graduating PhD student at the university of Bordeaux under the MSCA project DESTINY between "Institut de Chimie de la Matière Condensée de Bordeaux (ICMCB)" and "Laboratoire de Réactivité et Chimie des Solides (LRCS)". He received his BSc in Metallurgical Engineering from the Mindanao State University – Iligan Institute of Technology in 2015, and obtained a MSc in Resources Engineering under the



Cyril Aymonier

Cyril Aymonier is a CNRS senior researcher and the director of the "Institut de Chimie de la Matière Condensée de Bordeaux (ICMCB)". His current research interests are (i) the study of the chemistry and nucleation & growth in sub- and supercritical fluids applied to the design of advanced nanostructured materials, (ii) the investigation of material recycling using sub- and supercritical fluids and (iii) the development of the associated sub- and supercritical fluids-based technologies. He received the CNRS bronze medal, the Roy-Somiya award and the CNRS innovation medal for his scientific achievements.

## 1. Introduction

Since Sony introduced the first commercial lithium-ion batteries (LIBs) in 1991, these rechargeable energy storage devices have become an essential part of our daily lives. Initially developed for portable electronics, LIBs played a pivotal role in enabling the widespread adoption of smartphones, tablets, and laptops, revolutionizing our personal and professional lives. Over the years, continuous advancements in LIB performance, achieved through the discovery and optimization of new electrode materials, electrolytes, and improved industrial production processes, have significantly expanded their utility within the mobility sector. Fig. 1 illustrates the significant demand for LIBs, primarily driven by electric vehicles (EVs), and indicates a projected exponential increase in usage till 2030.

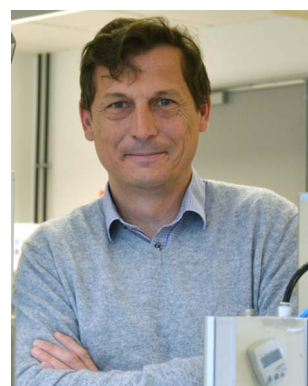


Laurence Croguennec

neutrons and synchrotron large scale facilities for *in situ* and *operando* characterization of battery materials during their operation. She is also actively involved in the French Network on the Electrochemical Energy Storage (RS2E) and in the ALISTORE European Research Institute devoted to battery research.

*Laurence Croguennec is a CNRS Research Director and the Deputy Director of the ICMCB. She has been working for 25+ years on crystal chemistry of electrode materials developed for metal-ion and all-solid-state batteries and the characterization of mechanisms involved upon cycling, especially for layered and spinel oxides and polyanionic-type positive electrode materials. She also collaborates with European*

This soaring demand for LIBs is closely linked to their cost, showing a remarkable decrease of over 80% in the price per kWh between 2013 and 2022 (Fig. 1). This drop can be attributed to economies of scale<sup>1</sup> driven by an increased and optimized LIB production and from the reduction and/or elimination of the use of expensive elements such as cobalt.<sup>2</sup> In addition, government incentive initiatives to EV buyers, offering premiums, tax reductions, and even exemptions, especially in Europe, have had a significant impact on the fast-growing LIB market.<sup>3,4</sup> For instance, automakers and the EV sector, one of the key stakeholders of LIBs, totaled more than 300 billion USD in investments in 2019, including Volkswagen, Daimler, Hyundai, Changen, Toyota, Ford, Chrysler, Nissan, Renault, BMW, Tesla, GM, GAC, Mahindra, and Great Wall.<sup>4</sup> Huge cell factories termed gigafactories are rapidly built all around the world; Tesla, Northvolt, CATL, SDI, LG Chem, Verkor, ACC, and



Mathieu Morcrette

*Mathieu Morcrette is a CNRS Research director at the CNRS and is currently the director of the Laboratoire de Réactivité et Chimie des Solides (UPJV, UMR CNRS 7314). Mathieu Morcrette's research is devoted to materials of today's Li-ion batteries, but also to the new generation of electrochemical energy storage systems such as Na-ion, Li/S or solid state technologies, through ANR or European projects. He also coordinates the activities of the pre-transfer units (Upscaling Materials, 18650 battery prototyping) of the RS2E (Réseau sur le stockage électrochimique de l'énergie) strongly involved in the development of the RS2E funded Tiamat company.*



Rémi Dedryvère

on chemical reactivity at materials surfaces and electrode/electrolyte interfaces, on passivation layers and aging mechanisms in Li-ion and post-Li-ion batteries.

*Rémi Dedryvère is Professor of materials chemistry at the University of Pau & Pays Adour (UPPA), in the Institute of Analytical Sciences and Physical Chemistry for Environment and Materials (IPREM). He received his PhD degree in 2000 from the University of Montpellier, France, and worked one year as researcher in the Georg-August University of Göttingen, Germany, before joining UPPA. His research activities are focused*



Jacob Olchowka

*Jacob Olchowka is a CNRS researcher at the ICMCB. After earning a joint PhD from the University of Lille (France) and the University of Siegen (Germany) in 2015, and a post-doctoral experience in Geneva, Jacob joined ICMCB, where his current research centers on the controlled synthesis of positive electrode materials for sodium-ion and lithium-ion batteries, as well as the development of innovative coatings to enhance material stability and performance. He is also actively engaged in Li-ion battery recycling research and is a member of the French (RS2E) and European (ALISTORE) research networks on batteries and energy storage.*

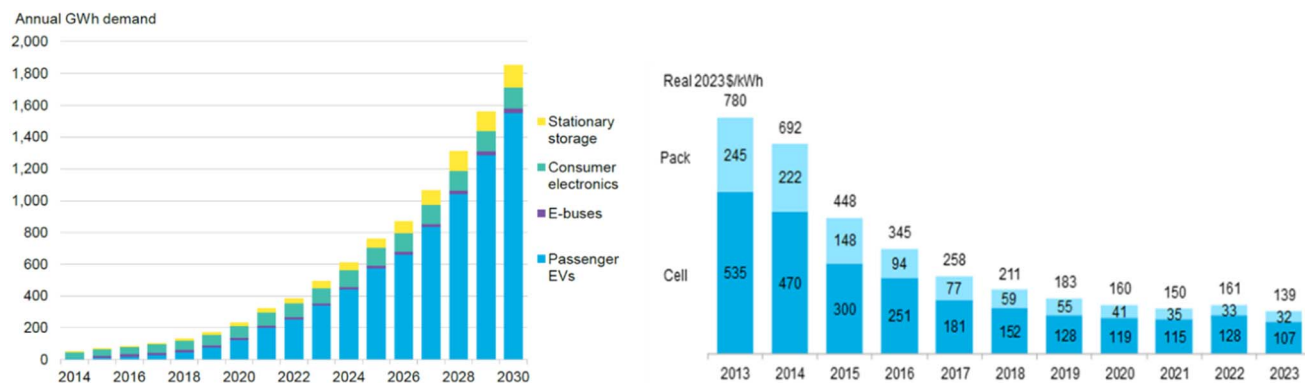


Fig. 1 Current and projected demand for the LIBs according to its application area (left) and evolution of a battery pack price superimposed to its cumulative demand (right) according to the BloombergNEF report.<sup>1</sup> Reproduced with permission from James Frith, BloombergNEF.

Table 1 Specific minimum recycling requirement and mandatory recycled content of LIB production as stipulated by (EU) No 2023/1542 (ref. 18)

	Now	2025	2027	2030	2035
End-of-Life LIB	Collection rate (%)	45%	65%	70%	
	Recycling efficiency (wt. %)	50%	65%	70%	
Battery composition	Material recovery (%)	Co, Cu, Ni	90%	95%	
		Li	50%	80%	
Recycled content (%)	Co			16%	26%
	Li			6%	12%
	Ni			6%	15%

many other companies are ready to produce and flood the market with batteries with a planned accumulated capacity of 600 GW h, which is only 40% of the projected demand in 2040.<sup>5,6</sup>

The electrification of mobility has resulted in a significant increase in the demand for raw materials used in battery packs.



Gilles Philippot

Gilles Philippot is an Assistant Professor at the University of Bordeaux. He obtained a PhD in Physical-Chemistry of Materials from the University of Bordeaux in 2014, working on the continuous solvothermal flow synthesis of metal oxide nanocrystals. Then he went to Aarhus (Denmark) for a one-year postdoctoral position to focus on the study of nucleation and growth mechanisms of nanocrystals formation in hydrothermal and solvothermal conditions, using *in situ* X ray scattering characterizations. He has been working on the synthesis of nanocrystals and the recycling of nanostructured materials using hydrothermal and solvothermal processes.

Compared to the relatively light batteries in smartphones (around 20–40 g),<sup>7</sup> EV battery packs can weigh between 300 and 900 kg.<sup>8</sup> This surge in demand puts pressure on the market for critical and strategic raw materials such as natural graphite, lithium (Li), cobalt (Co), copper (Cu), manganese (Mn), and nickel (Ni), as classified by the European Commission.<sup>9</sup> The first consequence of this phenomenon has already been observed, as for the first time in its history, the price of LIB kWh increased between 2021 and 2022 due to the increasing price of the raw materials (Fig. 1). Additionally, the growing EV market will lead to the production of a significant volume of battery wastes. Aside from batteries reaching their EOL (often called spent battery) and scraps<sup>10</sup> from their production, other LIBs retired due to declining performance which cannot support specific purposes such as those used in EV applications will quickly increase the rate of battery disposal. When an EV battery's capacity drops to 70–80% of its initial capacity,<sup>11,12</sup> it must be replaced. Although these used batteries can be repurposed for static energy storage in energy farms or grids, this second life will just delay their inescapable end of becoming wastes.<sup>11–15</sup> Thus, the need to develop efficient, scalable and low-cost recycling processes becomes vital to minimize raw material supply shortage as well as environmental and economic issues.

To achieve this challenge, there is an unavoidable starting investment cost to pay and, to push in this direction, several

countries and countries' associations have recently defined various binding directives. For instance, within the European Union (EU), the first directive 2006/66/EC<sup>16</sup> mandated to collect at least 45% of EOL LIB by September 2016 and stipulated that 50 wt% of these batteries must be recycled. The objective of this directive was to counter the disposal of waste batteries, thrown and landfilled or not recycled. However, this directive lacks the capacity in integrating technological advances and battery uses, besides its inadequate collection and low recovery rates. Consequently, the EU Committee on the Environment, Public Health, and Food Safety have recently repealed the Directive 2006/66/EC<sup>16</sup> with the newly approved and more rigid regulation: (EU) No 2023/1542.<sup>16-18</sup> Under this new regulation, new clauses include: new categories of EV and light means of transport (LMT) batteries; carbon footprint declaration; recycled content declaration; electrochemical performance and durability; battery replaceability; safety requirements; due diligence for third-party verification; and increased collection rates with specific material recovery targets (Table 1). It also highlights the second life of batteries, the need of a proper labeling for a better battery management system, and a battery passport for all commercial batteries. This recently approved regulation clearly suggests that recycling is not a stand-alone solution to LIB value chain. With this new regulation, especially in recycling and production, stakeholders are keener on developing, investigating, and improving ways to recirculate maximum materials back in the loop. Both these regulations do not suggest, identify, authorize, or mandate specific available technology for the recycling of batteries, they only promote LIB recycling. Therefore, political context joins the environmental

and economic ones to strongly push towards LIB recycling with a well-defined roadmap in terms of efficiency, while leaving the challenge to researchers and industry to develop and upscale such efficient recycling procedures for EOL LIBs.

Lastly, since 2010, the worldwide LIB community has been very active in this field as shown by a significant increase in the number of both publications and patents. Interestingly, 74% of the published literature for LIB recycling are patents, with annual volume growth of 32% for LIB recycling compared to 4% of all scientific chemical literature publication,<sup>19</sup> highlighting the emergence of this hot and new research topic.

### 1.1. LIB architecture

Before thinking on the ways to improve LIB recycling, it is primordial to know their architecture and composition to figure out what is to recycle. A LIB pack consists of multiple Li-ion cells connected in series and/or parallel to provide the required voltage and capacity. Commonly, there are three types of battery cells used on the market of EV batteries: cylindrical, prismatic, and pouch. Each format has its advantages and drawbacks when assembled in a battery pack, however, the architecture and the content within the different cell housings remain fundamentally similar. Fig. 2 shows the intricate details of an LIB 18650 cylindrical cell along with its complexities. This image represents the compact and complex linking of various components having different properties and attributes. A LIB cell is composed of a succession of double-side-coated electrodes, alternating positive and negative electrodes, which are separated by an ionically conductive membrane. A liquid electrolyte, which is a lithium salt dissolved in an organic solvent,

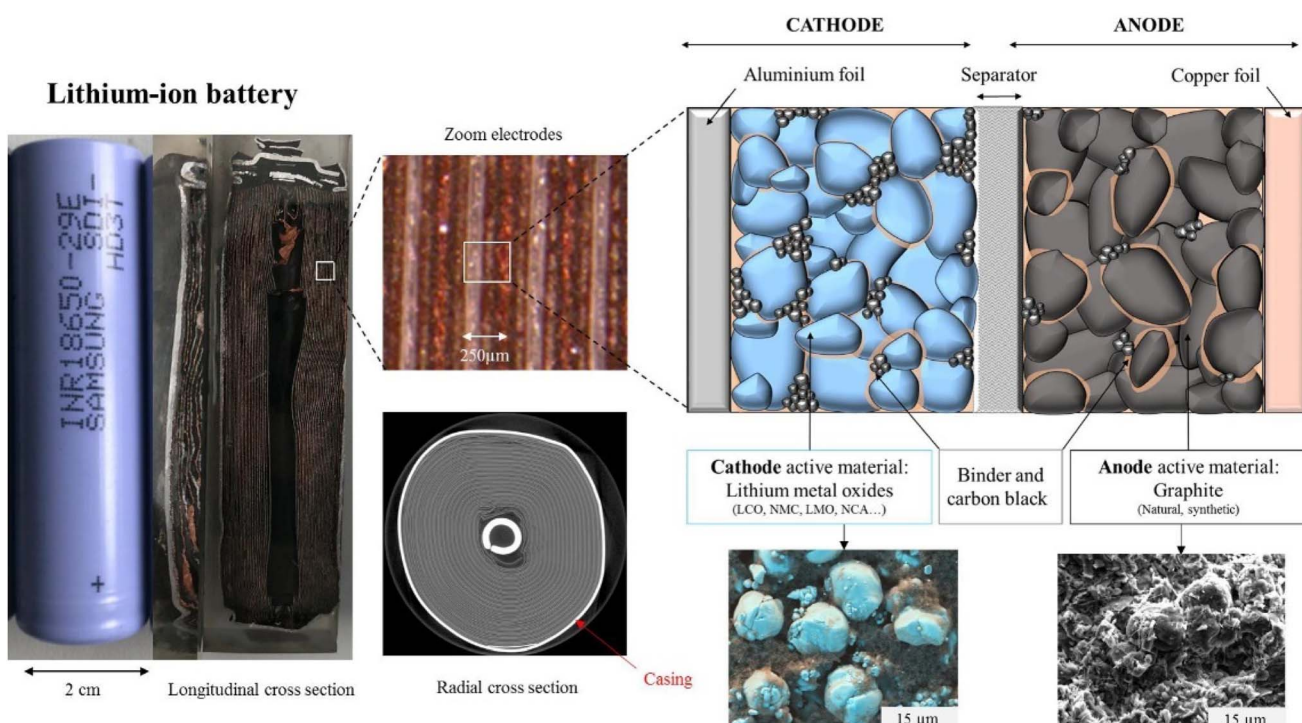


Fig. 2 Schematics of an 18650 battery highlighting the anatomy of a single LIB cell.<sup>20</sup> Reproduced with permission from Elsevier.

such as a mixture of ethylene carbonate and dimethyl carbonate, completes the device and the entire components are placed in a cell casing (metallic can in this case) and hermetically sealed.

Although the design of the positive and negative electrodes is relatively the same (a current collector in which a mixture containing active materials, binders and conductor additives is coated), they are significantly different in terms of chemical compositions for their various components. The positive electrode, often named as cathode, is made of an aluminum (Al) foil current collector where a mixture of active material, electronic conductive additive (usually carbon black, CB) and binder adheres. The chemical composition of the active material, which commonly represents a weight ratio of the mixture higher than 92%, varies depending on the Li-ion technology. NMC, NCA and LFP, which are  $\text{LiNi}_x\text{Mn}_y\text{Co}_z\text{O}_2$ ,  $\text{LiNi}_x\text{Co}_y\text{Al}_z\text{O}_2$  ( $x + y + z = 1$ ) and  $\text{LiFePO}_4$ , respectively, dominate the EV market, whereas other electrode material compositions such as  $\text{LiCoO}_2$  (LCO) are rather limited to smartphone applications. The exact nature of the binder polymer depends on the cell maker, but it is usually derived from polyvinylidene fluoride (PVDF). Furthermore, the negative electrode is composed of an active material, usually graphite or graphite–silicon, which is mixed with a conductive additive (CB) and a binder, and deposited on a Cu foil. Once again, the nature of the binder differs a lot

depending on the cell maker; however, carboxyl methyl cellulose (CMC) is among the most common ones paired with an adhesion aid of styrene butadiene rubber (SBR).

The battery pack also contains safety features such as a temperature sensor, a current limiter, a voltage cutoff to prevent overcharging or overheating and a battery management system (BMS) that monitors the voltage and temperature of each cell to ensure they are balanced and working properly. To summarize, a Li-ion cell and more widely a Li-ion battery pack are a complex assembly of a multitude of connections and materials such as plastics, metals, oxide (phosphate) materials, carbonaceous materials, various polymers and even liquids, which makes their recycling complex.<sup>21</sup>

## 1.2. State-of-the-art of current recycling approaches

When it comes to recycling, a unique methodology is demanding to be both cost-effective and efficient due to the complexity of a battery pack and the multitude of different components (Fig. 2). Therefore, a combination of mechanical, physical and chemical approaches is widely adopted to recycle spent LIBs. The usual and currently employed industrial recycling practice involves the combination of mechanical liberation followed by a chemical reaction initiated by pyrometallurgy and/or hydrometallurgy treatments. These recycling approaches aim at first, destroying all the components of the battery, and

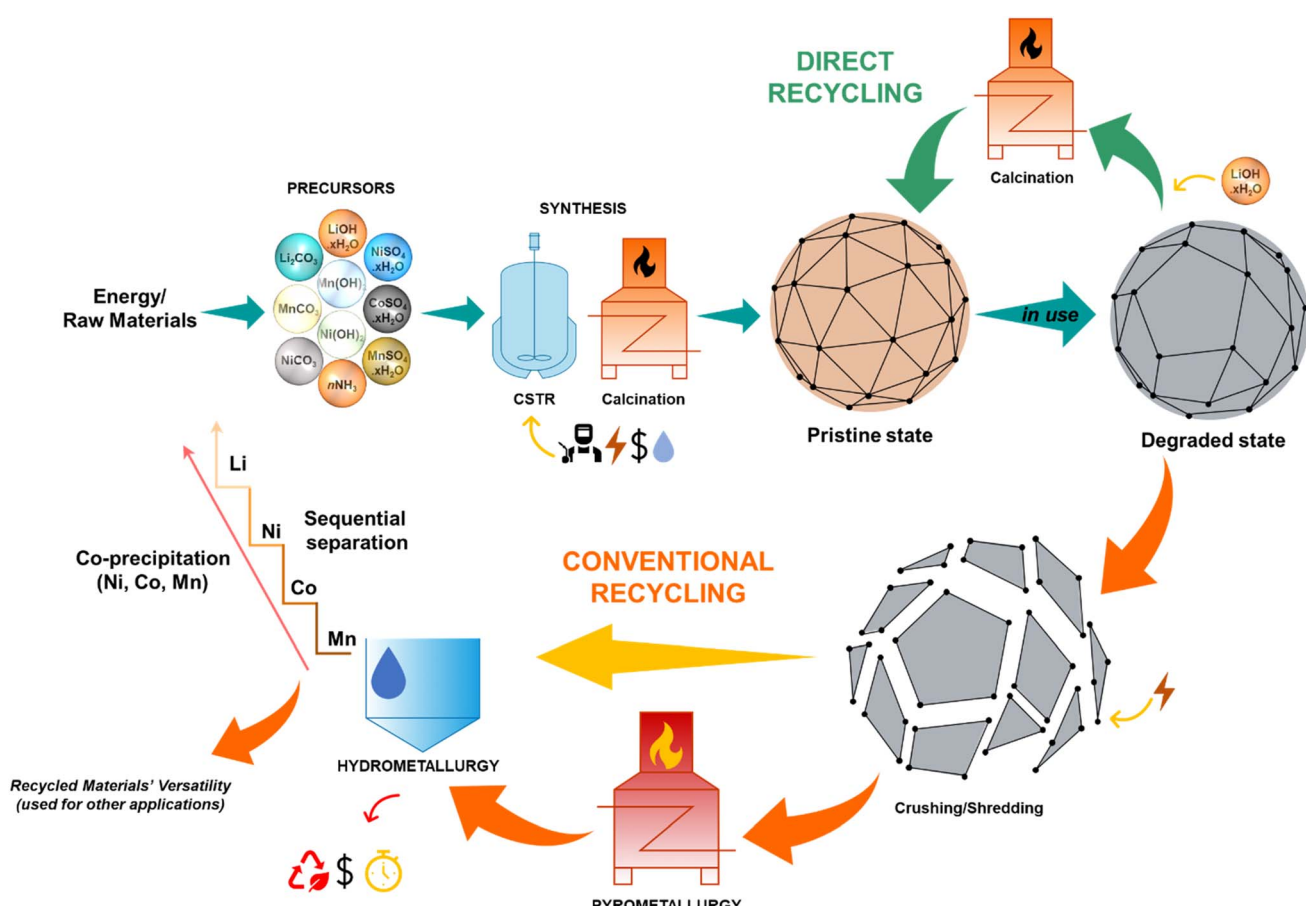


Fig. 3 Schematic of cathode active material recycling; comparing the conventional recycling process to direct recycling.

Table 2 Standard LIB recycling routes and their advantages and disadvantages highlighting some losses of components

Process	Advantages	Disadvantages	Ref.
Pyrometallurgy	No pre-treatments needed Low operational complexity Ease of scaling up No specific cathode chemistry Valuable only to recover Co, Cu and Ni	Electrolyte, binder, separator, and graphite are lost Partial recovery of Li and Al which are downcycled Energy intensive Generation of CO <sub>2</sub> , greenhouse gases, and toxic F-based gases Requires hydrometallurgy for purification and refinement of recovered metals	25, 27, 31 and 39
Hydrometallurgy	High selectivity High recovery High product purity Low energy consumption  Less gaseous wastes	Wastewater and water consumption Effluent toxicity Long process increases incurs loss of materials Requires efficient pretreatment and fine particles for faster dissolution kinetics  Electrolyte, separator and binder are lost	30 and 40

then, recovering the valuable materials elementally that become precursors. If the purity of the recovered elements is sufficiently high and reaches the so-called “battery grade”,<sup>22</sup> these recovered precursors are finally re-employed for the synthesis of new electrode materials that will be used to assemble new batteries. Otherwise, they can be used for other purposes requiring less rigorous purities, which is called downcycling. It is important to note that before recycling, the discharge of residual energy in EOL batteries is mandatory for safety purposes and a dismantling of battery modules is also performed to disconnect the various components such as cables, battery cells, frames, and electronics, which could be recovered.

Mechanical operation as a pre-treatment step employs crushing and grinding of a LIB for comminution or size reduction under both dry and wet conditions.<sup>23,24</sup> The product resulting from this step is the so-called “black mass”. Then, a secondary milling, which is highly energy intensive, can be applied to remove electrode composites (active materials, CB and binders) from their current collector metallic foils and unavoidably reduce foil sizes, transforming them in finer fractions.<sup>25</sup> The black mass therefore contains a mixture of various materials<sup>26,27</sup> and processing them for a specific target gets more complicated. In this step, no chemical alterations are made and all components of the battery cells are reduced in sizes, but their composition and state are relatively unchanged.

After the pre-treatment steps, separation utilizing pyrometallurgy and hydrometallurgy routes can produce refined quality metals, normally in their elemental states, chloride, sulfate, hydroxide or oxide forms. To make them economically viable, the costly transition metals drive these processes, as Co element, for instance. This is the reason why there is a huge gap of recycling processes, which is biased towards the cathode component.<sup>28</sup> However, the development of such methods faced huge challenges. Pyrometallurgy requires massive energy and additional treatment of the generated gases, as it contains fluorine from the electrolyte and the binder; Li is oxidized and joins the slag while graphite, binders, and electrolyte are not recovered.<sup>23,29,30</sup> Graphite acts as a reducing agent and is converted into carbon dioxide during the thermal treatment and is consequently lost. Additionally, the black mass, as it is

a mixture of materials, decreases the operation efficiency due to low overall reactivity, negatively influencing the melting point, slag viscosity, *etc.* Moreover, in pyrometallurgy, elements such as Al and Li can join the slag and ultimately get lost, resulting in a low yield<sup>31,32</sup> of about 70%.<sup>33</sup> Furthermore, in hydrometallurgy, dissolution and separation of metals are added challenges. This operation produces acidic wastewater that requires treatments and both the electrolyte and binder are lost most of the time during the pretreatments. In addition, its kinetics is dependent on the particle size, and thus, it is highly dependent on the pre-treatment.<sup>32,34</sup> Besides, there is an issue of reagent selectivity, for EOL NMC for example, the recovery of Ni, Mn, Co, and Li, which is affected by distribution coefficient, interruption of extraction, and the antagonistic effects of the elements<sup>35,36</sup> necessitates several steps (see Fig. 3). These two recycling methods are complementary and pyrometallurgy is often employed in combination with hydrometallurgy to attain a refined material and to reach a yield of about 90%.<sup>33</sup> Until now, there is no industrial scale facility able to recover the anode active material, the graphite. However, novel recycling routes are currently developed such as research studies conducted by Vanderbruggen *et al.*,<sup>20</sup> on the separation of anode active materials using their difference in surface properties implementing flotation. Graphite is considered a critical raw material also in EU; hence, its recovery is essential.

Dealing with the technical aspects, Sommerville *et al.*,<sup>27</sup> summarized some of the common pre-treatment methods, whereas Werner *et al.*,<sup>23</sup> published the common recycling steps in LIB chains such as waste logistics and presorting; pretreatment with the dismantling and depollution; processing with the liberation and separation; and lastly, metallurgy with the extraction and recovery. A lot has been recently published on these physico-chemical practices, confirming the booming research development in the LIB recycling field.<sup>21,23,26,27,29,30,34,37,38</sup> Industrial employment of these technologies is available worldwide such as in ACCUREC GmbH, Akkuser, Anhua Taisen Recycling Technology Co. Ltd, Batrec Industries AG, Düsenefeld GmbH, Li-Cycle US, OnTo Technology Oregon US, PROMESA GmbH & Co. KG, Recupyl S.A.S, Shenzhen Green Eco Manufacturer Hi-Tech. Co., Ltd, S.N.A.M., SungEel Hitech Ltd, Toxco/

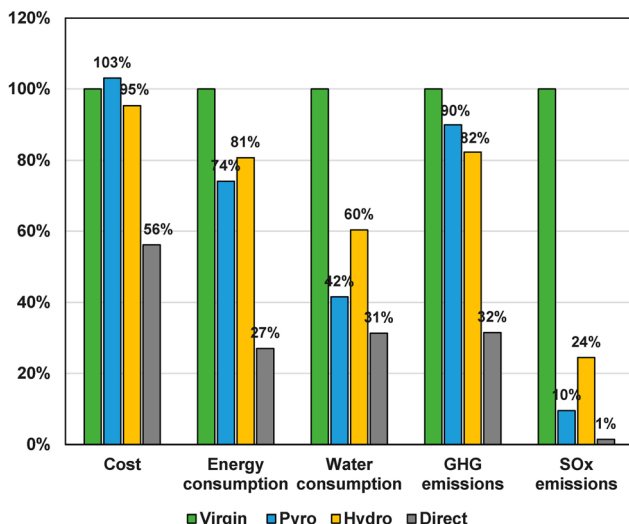


Fig. 4 Comparison of cost, energy, water and environmental impacts: greenhouse gas (GHG) and sulphur oxide (SOx) emissions of production and recycling of 1 kg NMC111 on large commercial scales (50 kT per year).<sup>41</sup> Reproduced with permission from MDPI.

Retriev, Umicore, REDUX GmbH, and S.N.A.M. However, the implementation of the above-mentioned recycling treatments comes with losses and disadvantages, as summarized in Table 2.

In hydrometallurgy and pyrometallurgy, the destruction of components down to their elemental form is very simple. However, implementing this traditional way of recycling incurs loss of time, energy, and money used during the production of these components. For example, battery material syntheses are very tedious and long, the equivalent energy used to make the well-defined crystal structure and microstructure is very high, and some cathode active materials (CAM) require calcination or annealing temperatures as high as 900 °C. These inputs in the production of active cathode materials are then lost, as the material is literally broken down to elemental form, on top of the additional energy required for its re-production from re-synthesis back to its precursors as battery-grade materials, making this method a very expensive option (see Fig. 3). Additionally, there is also an equivalent carbon footprint to be considered, which makes these methods less environmentally friendly. More importantly, implementing standard recycling is only feasible for Co-rich or Co and Ni-containing active materials due to their costs that are able to compensate the expensive processing cost and waste treatment steps. Hence, Co-free cathodes which are currently in rise, such as LiFePO<sub>4</sub>, are less prompt to be recycled in the traditional way because the operational costs are higher than the value of the recycled materials. New methods are thus sought and one of them is the direct recycling, which is well adapted to recycle both Co-containing and Co-free cathode materials.

Despite the non-negligible positive aspects of pyro- and hydrometallurgy, the various limitations described in Table 2 justify an inevitable need to develop new and/or complementary approaches to meet the expectations in the domain of LIB

recycling, especially to narrow the increasing gap between the demand and supply of raw materials, which are becoming a critical issue, while remaining economically and environmentally viable.

## 2. Direct recycling: an alternative and promising approach

To increase the recycling efficiency, practices that only focus on specific or valuable elements should be avoided. Recycling should look at least at the component-based level or at the entirety of the LIB, and this is where a new recycling strategy is now gaining interest, the direct one. Direct recycling is a non-destructive approach that aims to separate and recover the different components of the electrochemical cells, *i.e.* current collectors, cathode and anode materials, binders, electrolytes, *etc.*, and re-use them into a new battery after purification, cleaning and/or regeneration. This new approach attracts considerable attention, not only due to its possible huge environmental and economic benefits (Fig. 4), but also because the regulation objectives now appear to be more reasonably reachable. Indeed, enabling direct reuse in battery manufacturing results in reduction of time, operating cost, and environmental impacts.<sup>32,42,43</sup> Practically, all components are recoverable by direct recycling,<sup>44,45</sup> resulting in a more value-adding process. Lastly, the economics of direct recycling does not depend on battery chemistry. To summarize the advantages of direct recycling over standard methods, Argonne Lab with its Everbatt model compared LIB recycling in different routes. As presented in Fig. 4, direct recycling of NMC111 exhibits advantages in all the listed major key parameter indicators: cost, energy, resource consumption, and emissions.

Despite the advantages of direct recycling, F. Larouche *et al.*<sup>43</sup> reported that direct recycling is sensitive to parameters such as battery type, accumulation of defects and impurities, cell composition, state of health, market variation, and even the development of new battery chemistries. These disadvantages are especially applicable to EOL LIBs. On the contrary, this new method of recovering materials from LIB cells is remarkable, especially in the case of production scraps<sup>10</sup> where all these characteristics are known and mastered.<sup>46</sup> It can pave the way in increasing the recycling efficiency and recovering the largest portion of cathode and anode's value by preserving their composition and structure, away from destructive methods currently employed. Thus, to have a possible large-scale application, it is important to develop direct recycling approaches and robust processes that encompass the recycling of broad range of battery technologies, and even beyond Li-ion ones to anticipate the future energy storage generation devices (*e.g.* Na-ion batteries).

The majority of the research papers and existing reviews dealing with direct recycling focus on the recovery/regeneration of the positive electrode material, whereas the other components of the battery cells are often overlooked. In order to extend the direct recycling on the battery cell scale, this review paper discusses the various component-based direct recycling

**Table 3** Electrolyte recovery with liquid and supercritical CO<sub>2</sub>. (N.D.: not disclosed but mentioned; N.R.: not recovered; ACN: acetonitrile; and PC: propylene carbonate)

Electrolyte composition	Sample	Cosolvent	Temp. (°C)	Pressure (bar)	Time (min)	Li salt recovery	Extraction yield, %	Ref.
1.2 M LiPF <sub>6</sub> in (1 : 1% wt) EC : DEC	Prismatic cells	N.D.	50	283	120	N.D.	92	71
1 M LiPF <sub>6</sub> in (1 : 1 : 1% vol) EC : DMC : EMC	Polypropylene separator	—	40	230	45	Low	85.1 ± 0.4	72
1 M LiPF <sub>6</sub> in (1 : 1 : 1% vol) EC : DMC : EMC	Polypropylene separator	—	50	350	45	N.R.	88.7 ± 0.9	73
1 M LiPF <sub>6</sub> in (1 : 1% wt) EC : DMC	Polyethylene fleece	—	40	120	90	High	73.5 ± 3.6	74
1 M LiPF <sub>6</sub> in (1 : 1% wt) EC : DMC	Porous glass fiber	—				—	36.75 ± 1.6	
1 M LiPF <sub>6</sub> in (1 : 1% wt) EC : DMC	18650 cells	—				N.D.	N.D.	
1.1 M LiPF <sub>6</sub> in (1 : 1 : 1% vol) EC : DMC : EMC	18650 and pouch cells	(3 : 1) ACN : PC	25	60	50	High	89.1 ± 3.4	75

routes currently developed. As such, the structure of this review paper includes the recovery/recycling of the main components of LIBs: electrolyte, positive electrode, and negative electrode. It aims to provide a holistic and critical overview of the state-of-the-art LIB direct recycling. The specific targets of this review article are: (1) to propose a comprehensive review on the available direct recycling technologies for the LIB while considering all its main components, from the active materials to the non-electrochemically active components such as electrolyte; and (2) to show applicability and limitations for different LIB technologies within the concept of circular economy. Within this framework, the details of each process for specific LIB components are described. The details on cost savings and environmental impacts of the listed processes are not the focus of this paper. In this review paper, diverse battery active materials are presented.

### 3. Specific treatment of each component

#### 3.1. Electrolyte recovery

In an LIB assembly, the electrolyte acts as an ionic conductor that transports Li<sup>+</sup> ions between electrodes during the charge and discharge processes. Although it can sometimes be a ceramic or a polymer, in a large majority of LIBs, the electrolyte is an organic mixture of solvents in which lithium salt is dissolved, and is the only liquid component in the cell.<sup>47–50</sup> The most common commercial liquid non-aqueous electrolyte, used for LIBs, contains a lithium salt dissolved in a mixture of cyclic carbonate solvents – ethylene carbonate (EC) and/or propylene carbonate (PC) – and linear carbonate solvents – dimethyl carbonate (DMC), ethyl methyl carbonate (EMC) and/or diethyl carbonate (DEC).<sup>50,51</sup> The most widely used salt is the lithium hexafluorophosphate (LiPF<sub>6</sub>), but other salts such as LiAsF<sub>6</sub>, LiBF<sub>4</sub>, LiClO<sub>4</sub>, LiBETI, and LiTFSI also exist.

The electrolyte represents 10–15 wt% of the LIB assembly<sup>52</sup> and around 10% of material costs.<sup>53</sup> For instance, Susarla *et al.*<sup>49</sup> evaluated the cost of producing LiPF<sub>6</sub> at 20 USD per kg for a facility with an annual production of 10 000 tons, which is in good agreement with the previous estimations made by Patry *et al.*<sup>54</sup> Electrolyte recycling is highly attractive from an

economic point of view as its price gained a +135% increase from January to September 2021.<sup>55</sup> In addition, its production utilizes an annual energy consumption of 30 GW h and CO<sub>2</sub> emission of 80 tons per day for 10 000 tons of LiPF<sub>6</sub> annual production.<sup>49</sup> For all these reasons, the electrolyte requires attention for recycling.

Once the battery is assembled and the electrolyte is added, the contact of electrolytes and electrodes leads to the initial LiF formation, resulting from the Li salt chemical degradation. During its use, the electrolyte degrades through different mechanisms that can be induced by chemical, electrochemical and/or thermal stress.<sup>48,51,56–61</sup> During the first charge or formation cycles, the decomposition products stemming from the electrochemical degradation of electrolyte contribute to the formation of the solid electrolyte interphase (SEI) at the negative electrode surface, and a different kind of passivation layer at the positive electrode surface, which is often called the cathode electrolyte interphase (CEI).<sup>62–64</sup> It has to be noted that CEI and SEI's composition highly depends on the nature of aging or the use phase of batteries. Besides, temperature-induced degradation of the electrolyte can occur during

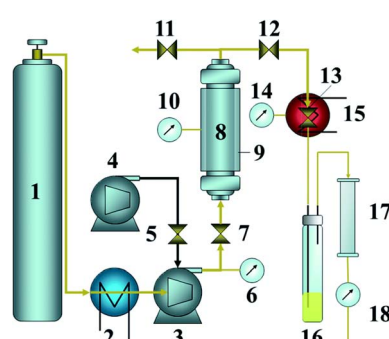


**Fig. 5** Common set-up for electrolyte extraction with liquid and supercritical CO<sub>2</sub>.<sup>72</sup> The set-up contains (1) CO<sub>2</sub> cylinder, (2) cooling bath, (3) air-driven fluid pump (gas booster pump), (4) air compressor, (5) air regulator, (6) CO<sub>2</sub> pressure, (7) inlet valve, (8) extraction vessel (reactor), (9) heating jacket, (10) vessel heat, (11) vent valve, (12) outlet valve, (13) flow valve, (14) valve heat, (15) heating jacket, (16) collecting vial, (17) alumina filter, and (18) gas flow meter. Reproduced with permission from RSC advances.

battery storage especially at the charge state or during regular aging and utilization, indeed the electrolyte combusts at 300 °C.

With respect to LIB recycling, most methods do not recover the electrolyte. However, the removal of electrolyte is essential to avoid the jeopardy of the equipment due to its corrosive nature<sup>23</sup> and to ensure operator's safety.<sup>65</sup> The degraded electrolyte is usually removed based on thermal treatment (120–600 °C), such as calcination and pyrolysis,<sup>66,67</sup> which is associated with energy consumption, environmental, safety, and economic issues. Dealing with the electrolyte salt, Zhao *et al.*<sup>68</sup> mentioned that LiPF<sub>6</sub> decomposes into LiF and PF<sub>5</sub> at 60 °C (90 °C at 300 ppm H<sub>2</sub>O<sup>69</sup>) and hydrolyzes to HF in the presence of water, thus air exposure and water must be both avoided during battery assembly and disassembly. Without the presence of water, the LiPF<sub>6</sub> salt is, at room temperature, in equilibrium with its decomposition products LiF and PF<sub>5</sub> and degrades just below 70 °C.<sup>65</sup> Therefore, the salt recovery must be done at a rather low temperature. Additionally, the fluorine content found in the electrolyte salt (and also in the positive electrode binder) suggests expensive waste gas treatment because it poses risks to people and environment.<sup>41,70</sup> Hence, as presented in Table 3, the employed electrolyte extraction temperature only reaches to a maximum of 50 °C. While the specific technique is commonly called supercritical fluid extraction, the technique is more accurately described as using pressurized fluids. In fact, pressurized CO<sub>2</sub> in its liquid form appears to work better than scCO<sub>2</sub> in terms of recovery and yield.<sup>74</sup> Besides, as investigated by Rothermel *et al.*,<sup>76</sup> the use of scCO<sub>2</sub> negatively affected the crystal structure of graphite, the anode active material. Finally, to qualify for the direct recycling of LIBs, the electrolyte must be extracted out of the cell during the processing. The only method applied for electrolyte recycling is based on its extraction using liquid or supercritical CO<sub>2</sub> added with organic cosolvents. The common set-up to conduct this extraction is shown in Fig. 5 with the description of the different parts in the caption. The CO<sub>2</sub> allows dissolving and extracting the electrolyte, which can be recovered at the end of the process. Lastly, CO<sub>2</sub> can either be compressed and used again or discharged. A summary of data extracted from works using the CO<sub>2</sub>-based extraction technique is given in Table 3.

Sloop & Parker<sup>71</sup> patented the use of supercritical CO<sub>2</sub> (scCO<sub>2</sub>) for the extraction of electrolytes from LIBs (see Table 3). A fully discharged battery is placed in a reactor, CO<sub>2</sub> is added, heated and pressurized beyond the critical point (*T*, *P*); the extracted electrolyte is then collected and CO<sub>2</sub> is recycled. This patent paved the way for using supercritical fluids for EOL LIB electrolyte extraction. The results showed that at ambient temperature, 71% of the electrolyte could already be recovered in 10 minutes. This patent did not disclose if the salt, LiPF<sub>6</sub>, is recovered during the experiment but only mentioned that the mixture of EC/DEC/LiPF<sub>6</sub> resulted in a total recovery yield of 92% after two hours of processing. This success is attributed to the properties of CO<sub>2</sub> above its critical point. Apart from the electrolyte, CO<sub>2</sub> can also remove the oligocarbonates and ethers from the electrodes' surface and other degradation products accumulated during the lifetime of the battery. However, it did not show the possibility of re-using the recycled electrolyte

again in an LIB nor the separation of each carbonates. Furthermore, the investigation of the effects and impacts of the process on the other components such as the cathode and the anode of LIBs was not mentioned. Sloop's patent<sup>71</sup> provided a good insight on a new technology that ignited the research of electrolyte recovery, a component often overlooked in LIB recycling. This patent was then improved methodically through various studies such as the published outputs of Grützke *et al.*<sup>75</sup> and Liu *et al.*<sup>73</sup>

Grützke's<sup>75</sup> team studied the electrolyte extraction in both commercially sold 18650 (CGR18650CH Li-ion MH12210 Panasonic) and pouch cells made of LiNi<sub>1/3</sub>Co<sub>1/3</sub>Mn<sub>1/3</sub>O<sub>2</sub> (NMC111)/graphite. They evaluated the variation of flow rate and pressure on the extraction process. The increase in CO<sub>2</sub> flowrate at the same pressure and duration resulted in higher recovery rates. However, the experiments of varying the pressure of 80 vs. 300 bar at a temperature of 40 °C showed only a slight difference in recovery. The highest recovery of 89% was obtained with 30 min process in liqCO<sub>2</sub> (25 °C and 60 bar), followed by co-flowing (0.5 mL min<sup>-1</sup>) 3 : 1 ACN/PC and CO<sub>2</sub> streams and lastly with 20 min of only liqCO<sub>2</sub>.

The initial patent of Sloop & Parker<sup>71</sup> reports a yield recovery of 92% as presented above in Table 2, with 71% and 76% of electrolyte already recovered in 10 min using pure CO<sub>2</sub> in liquid and supercritical state, respectively. Conversely, the recovery reported by Grützke's is limited to 50% for 20 min when using liqCO<sub>2</sub> and even lower under supercritical conditions, which could be due to the possible decomposition of LiPF<sub>6</sub> above 55 °C. Besides, they found that EC is recovered better in scCO<sub>2</sub> than in liqCO<sub>2</sub>, as revealed through electrolyte component analysis. It was attributed to the dipolar moment of EC, which is much higher than that of DMC and EMC. The implementation of liqCO<sub>2</sub> was further investigated to increase the recovery reaching 89 wt% (LiPF<sub>6</sub> included) by adding cosolvents such as acetonitrile (ACN), diethyl carbonate DEC and 3 : 1 ACN : propylene (PC), as shown in Table 3.

Liu *et al.*<sup>73</sup> also investigated the use of scCO<sub>2</sub> to recover LIB electrolytes as a proof of concept. The experiments were performed with a laboratory-prepared electrolyte containing 1 M LiPF<sub>6</sub> with 1 : 1 : 1 by a volume mixture of EC, DMC, and EMC and extraction tests were done on polypropylene separators impregnated with 2 g of this mixture. Variables included pressure (150–350 bar), temperature (30–50 °C) and extraction time (25–65 min). The study found that the increase in pressure from 150 to 350 bar only improved the extraction by 5%, with a higher pressure favoring the EC recovery. DMC and EMC were fully extracted at 150 bar within 6 min, while EC required 12 min and higher pressure to reach 90–98% recovery. Higher temperatures decreased the EC recovery from 95% to 89%, but increased DMC and EMC. Lastly, the extraction efficiency improved with time from 83% at 25 min to 87% at 65 min. The study suggests that a medium polarity cosolvent is needed for the EC recovery. Despite these good results, it is worth noting that these results were obtained with the electrolyte with no side impediments such as decomposed electrolyte or real challenges to extract impregnated electrolyte within the active material's voids. Nevertheless, this work can be used as a guideline for

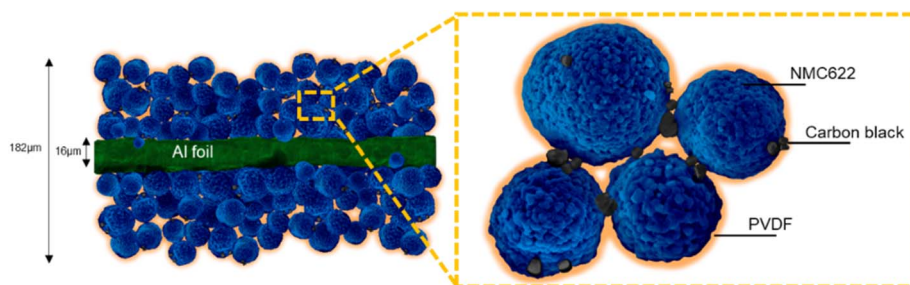


Fig. 6 Positive electrode schematic description highlighting the details of the active material, PVDF, and carbon black.<sup>46</sup>

optimizing experimental parameters in using  $\text{CO}_2$  for electrolyte extraction.

This first part on electrolyte recovery showed the effective demonstration of electrolyte recycling from LIBs by using liq $\text{CO}_2$  and sc $\text{CO}_2$ . Previously, the electrolyte was deemed a threat to the environment, to the equipment in recycling, and to the operators. These papers added way to electrolytes' valorization and showed the possibility for their recovery and potential re-use, leading to an increase in recycling efficiency of LIBs. Indeed, the effective re-use of recycled electrolytes into new batteries has yet to be demonstrated, to validate the methods just discussed. To the best of our knowledge, no one has directly re-used any recovered electrolyte even on a lab-scale. Lastly, the comparison of the state and conditions of degradations of the other battery cell components, before and after the electrolyte extraction, must be investigated for real-life purpose as the full picture of a Li-ion cell has to be considered.

### 3.2. Positive electrode delamination, separation, and regeneration

Fig. 6 shows the schematic description of a positive electrode, containing the active material (NMC622), CB, and PVDF binder coated on an Al foil. Among its different components, the positive electrode material or cathode active material (CAM) has attracted considerable attention in all the recycling operations due to its high value, and is usually the first component in LIBs targeted to be recycled. The most commercially available materials are the LFP, NMC, LCO, NCA, and Lithium Manganese Oxide ( $\text{LMO}-\text{LiMn}_2\text{O}_4$ ). Some of these materials have different variants according to transition metal ratios such as the NMC, which is available as NMC111, NMC532, NMC622, or NMC811. In the current landscape, there is a focus on Ni-rich materials due to the correlation between higher Ni content and increased specific capacity.<sup>77</sup> Additionally, considering that Co is costlier than Ni and Mn, reducing or eliminating its usage also brings about significant economic benefits. Dealing with cost-benefits, the use of LFP electrode materials and their derivatives  $\text{LiFe}_{1-x}\text{Mn}_x\text{PO}_4$  for mobility purposes strongly increased in the past few years due to the low price of Fe and Mn raw materials and progresses in the battery cell manufacturing allowing to reach acceptable volumetric energy densities. However, the recycling of such cost-effective electrode materials can present some challenges due to the low market value of the recovered elements, making possibly the traditional recycling

process more expensive than the mining and fabrication of new materials. Thus, the direct recycling for such type of electrode materials seems to be the only possible approach to minimize the costs and to meet the regulations concerning EV batteries.

One of the biggest challenges in the direct recycling of positive electrodes is the effective delamination of the active materials from the Al foil; especially focusing on cost-effective and more environmental options. Notably, the main objective of direct recycling is centered around the retrieval of materials without further damages or destroying them, seeking instead their regeneration for potential re-use. The challenge here is to loosen the adhesive and cohesive force of the binder, usually PVDF, to liberate the composite material (CAM, binder, and electronic conductor additive) from the current collector, while safeguarding its intrinsic characteristics and properties. More globally, due to the delamination of the electrode composites, all the active materials, binders, electronic conductor additives and foils can be recovered with appropriate methods and potentially reemployed in LIBs. Therefore, there are at least two steps in the direct recycling of the positive electrode, namely, (1) delamination-separation process, and (2) the subsequent regeneration of the CAM. The following part aims to provide a critical overview of both delamination and electrode material regeneration approaches that have been studied and reported in the literature.

**3.2.1. Different strategies on positive electrode delamination.** There are three main general methods for the delamination of the positive electrode employed for a PVDF-based binder. These methods encompass thermal, mechanical, and chemical approaches. The polymer binder serves as a crucial component responsible for holding together the active materials and conductive additives. Its primary role is to create a cohesive structure that maintains the integrity of the electrode while allowing for efficient electron and ion transport during the charge and discharge cycles in a battery. PVDF is inexpensive and cost-effective compared to other polymers. Moreover, although it possesses a limited ionic conductivity, it has high chemical resistance and good electrochemical stability, making it a good binder for the positive electrode. Conversely, the strong binding power of PVDF makes the delamination difficult. The three effective approaches for the purpose of delamination are presented below.

*(a) Thermal decomposition-based separation.* The thermal treatment methodology is based on the decomposition of the PVDF binder. This serves to lessen or eliminate the adhesive

and cohesive forces linking the binder to the CAM and electronic conductor additives, as well as the binder to the Al foil. Selective decomposition of PVDF is feasible due to its lower decomposition temperature at 440 °C than CAM, graphite, carbon black, Al and Cu foils<sup>25</sup> especially for the processes targeted on whole batteries; in this case, the thermal runaway is to be considered in process design.

A more favorable approach involves vacuum pyrolysis, primarily due to the entrapment of the evolved gases, which are potential pollutants.<sup>39</sup> Nevertheless, other interesting thermal delamination methods are also explored by Lee & Rhee,<sup>78</sup> Lu *et al.*,<sup>79</sup> and D. Song *et al.*<sup>80</sup> Vacuum pyrolysis involves a slow heating process at 10 °C min<sup>-1</sup> with a long contact time of the solid residues inside a reactor and a short residence time of the condensable organic vapors formed during the reactions, which minimizes the secondary decomposition reactions.<sup>39,81,82</sup> In this process, organic materials are decomposed to low molecular products without oxygen such as gases and oils from the decomposition of the binder and the electrolyte.<sup>39</sup> Because of this phenomenon, the positive electrode material peels-off from the Al foil and could be recovered. The set-up is under vacuum and so the toxic gases are trapped and collected, and the decomposition temperature of the organics is lowered. The current collector and the cathode active material, which are the main products, are not oxidized even at high temperatures, while the electrolyte and PVDF decomposition products could be collected. For instance, Sun & Qiu *et al.* (2011)<sup>83</sup> heated the electrodes at 600 °C for 30 min at below 1 kPa for such purposes.

Hanisch *et al.*<sup>25</sup> developed the adhesion neutralization *via* incineration and impact liberation (ANVIL), a two-stage process. First, the adhesion between the electrode's components is neutralized, which was conducted for a scrap NMC111 electrode with heating at 500 °C for 90 min. Then, an impact is applied for 1 min using an air jet to de-agglomerate the composite material, and the recovered composite powder is sieved only for size classification and not for component separation. This combination results in a delamination efficiency of 97%.

While one might think of heating PVDF for delamination, lower temperature processes such as cryogenic operations are also performed;<sup>84,85</sup> this maximizes the change in the adhesive

property of the PVDF, which is presented in the subsequent section. One main limitation of the thermal treatment, beyond the fact that the binder cannot be recovered, is the emission of toxic gases, requiring thorough scrubbing or trapping. Another problem with thermal treatments is that after the decomposition temperature of PVDF at 440 °C, a stable residue is formed.<sup>86</sup> Furthermore, the thermal method is constrained by the Al melting temperature, which is at around 600 °C and could lead to a potential reaction of the electrode material with the polymer during its decomposition. Besides, high-temperature treatment might cause some active materials to change in their composition, structure and microstructure, which further alters the energy storage performance. For instance, partially delithiated layered NMC can undergo phase transition to rock salt or spinel-type compounds at a temperature lower than that of PVDF decomposition, which would prevent further direct recycling.

(b) *Mechanical delamination.* Mechanical delamination methods such as crushing and grinding are widely used as pre-treatment steps for LIB recycling,<sup>23</sup> mainly for size reduction. An investigation conducted by T. Zhang *et al.*<sup>24</sup> encompassed both wet and dry crushing of LIBs. Wet crushing was performed with a blade crusher added with water. During the process, the blades rotate freely inside the crusher imparting kinetic energy and fracturing the electrodes. Besides, particle-to-particle crushing occurs when they come into contact, especially at high speed. The wet crushing produces a slurry, subsequently sieved to segregate the sizes. In contrast, dry crushing involved shear crushing followed by impact crushing and sieving. Generally, the resulting particle size distribution is coarser, falling in the millimeter range. This means that the positive electrode components presented in Fig. 6 are not separated.

Depending on the delamination temperature, the mechanical and physical properties of interfaces change, hence, H. Wang *et al.*<sup>84</sup> and Liu, *et al.*<sup>85</sup> performed cryogenic grinding. They observed a transition of PVDF from elastic to glassy state at low temperatures, thereby weakening the binding properties. The experiments were carried out with a cryogenic ball mill aided with liquid nitrogen, achieving a temperature of -196 °C. The obtained results were about 87% delamination compared to 25% at room-temperature experiments.

**Table 4** Hansen solubility parameters (MPa<sup>1/2</sup>): with details of energy from dispersion ( $\delta_d$ ), intermolecular ( $\delta_p$ ), and hydrogen bonds ( $\delta_H$ ) for the most widely used solvents in the chemical delamination of positive electrodes and their melting, boiling and flash points (°C)

Compound	$\delta_d$	$\delta_p$	$\delta_H$	$T_{\text{melting}}$	$T_{\text{boiling}}$	Flash point	CAS No.
PVDF	17.2	12.5	9.2	177			24937-79-9
NMP	18.4	12.3	7.2	-24	204	91	872-50-4
Cyrene	18.7	10.5	6.9	-20	227	108	53716-82-8
Acetone	15.5	10.4	7.0	-95	56	-17	67-64-1
TEP	16.8	11.5	9.2	-56	216	115	78-40-0
DMF	17.4	13.7	11.3	-61	153	58	68-12-2
DMSO	18.4	16.4	10.2	19	189	87	67-68-5
DMAc	16.8	11.5	9.4	-20	166	64	127-19-5
DMI	17.6	7.1	7.5	-70	94	108	5306-85-4
EG	17.0	11.0	26.0	-13	197	115	107-21-1

Electrohydraulic and electrodynamic (electro-mechanical) fragmentation introduces high-voltage pulsations as a new delamination technology.<sup>87,88</sup> This process entails immersing the electrode in a medium, typically water, and subjecting it to a substantial amount of energy (20–35 kV) in a very short time. This method provides the disintegration of complex composite materials at their interfaces.<sup>89</sup> Indeed, the shockwaves attack on the sample's weakest points, which are the mechanical bonds between grain boundaries and between different types of materials. With the energy added to cause the delamination, a subsequent local heating of the system is observed. Although Tokoro *et al.*<sup>87</sup> obtained 94% of delamination, Al foil contamination was observed with the recovered positive electrode material. This method could effectively delaminate the positive electrode; however, the possibility of reaction between the CAM and the water could potentially alter its composition.

One of the main disadvantages of implementing mechanical delamination is the presence of undissolved or undecomposed binders, persisting with the Al foil and on the surface of active particles even after delamination, which makes the component separation difficult and hence, the downstream process challenging. Moreover, depending on the mechanical energy, it is possible to alter the quality of the active materials in terms of (i) morphology with a loss of microstructure, (ii) crystal structure with potential amorphization and/or reaction with the binder and/or electronic conductor additive due to the high input energy and (iii) purity with potential contaminations from the grinding tools themselves.

(c) *Chemical dissolution.* The chemical approach to delamination involves the utilization of solvents and other media at low to mild temperatures to selectively dissolve the binder. It makes the compatibility of the solvent's solubility parameter with the binder a key consideration. Dealing with the PVDF binder, in addition to *N*-methyl-2-pyrrolidone (NMP) employed to prepare the slurry during electrode's manufacturing, various other organic solvents (see Table 4) such as triethyl phosphate (TEP), dihydrolevoglucosenone (cycrene), ethylene glycol (EG), dimethylacetamide (DMAc), dimethylformamide (DMF), and dimethyl isosorbide (DMI) are known to dissolve this polymer. Additionally, ionic liquids, molten salts and deep eutectic solvents are explored for this purpose. Recently, Hayagan *et al.*<sup>46</sup> have provided a list of some examples of chemical delamination methods applied to PVDF-based positive electrodes.

For instance, Buken *et al.*<sup>90</sup> employed DMI to recover the active material and the Al foil from a homemade positive electrode and an EOL 18650 Samsung battery. The DMI solvent reduces the polymer interchain interaction through penetration in the binder crystalline region. It was observed that the binder within the homemade cathode soaked in 40 mL DMI per gram of electrode and heated at 150 °C is dissolved within 30 minutes while five hours are needed to dissolve the binder of the EOL battery for the same amount of electrode. This experiment resulted in partial delamination of the CAM from the Al substrate only, requiring further ultrasonication followed by washing using diethyl ether to optimize the process. The recovered powder still contained the conductive carbon but the EOL electrode material displayed consistent surface

morphologies comparable to pristine materials. However, traces of phosphorus (P) were detected in the EOL material using EDS, suggesting the presence of residual electrolyte salt, LiPF<sub>6</sub> or its decomposition products. The industrial battery contained a mixture of CAM: LMO, LCO and NMC111, which added difficulty in determining the changes in the particle size due to the treatment. To compensate the lack of data, a homemade NMC111 underwent the same experiment revealing the preservation of its crystal structure as well as no changes within particle morphology, which confirmed the promise of this direct recycling operation. Despite these encouraging results, the electrochemical performance of the recovered materials was not tested to fully validate the efficiency of this approach.

A more rapid solvent-based delamination process was reported by Bai *et al.*<sup>91</sup> using ethylene glycol on NMC532 and NMC622 scrap trimmings. Successful outcomes were achieved at 160 °C with a 1 : 10 solid-to-liquid weight ratio under stirring conditions. In this work, pre-washing with dimethyl carbonate was performed prior to operation, while a post-rinsing for the Al foil and CAM using ethanol was applied to remove EG residues. The temperature has a major impact on the delamination time; it only takes 2 minutes at 100 °C, 6 seconds at 160 °C, and as fast as 2 seconds at 198 °C. However, it was found out that a loss of Li content was encountered from its initial value of 1.015 down to 0.993 after EG treatment and it revealed that the binder was not completely dissolved using EG.

In another study, Bai *et al.*<sup>92</sup> observed that no lithium leaching was detected when using triethyl phosphate (TEP) as a solvent, contrary to their previous work with EG. The method also proves that direct recycling has 100% efficiency of the positive electrode material, Al foil, and introduces the possible recovery of the binder in both spent LIB and NMC622 scrap trimmings. The recovered electrode material from scrap revealed a specific capacity at C/10 of 177.4 mA h g<sup>-1</sup>, which is slightly lower than that of their reference 186.5 mA h g<sup>-1</sup> due to the presence of residual PVDF (0.41% wt) and carbon black (1.79% wt). Nevertheless, this result demonstrates that 95.5% of initial capacity was recovered and that the process did not significantly degrade the material performance. For the NMC622 electrode scrap, the delamination procedure was conducted at 100 °C under stirring condition in TEP. Furthermore, mechanical stirring is not enough for the cathode recovered from spent LIBs. Hence, it was delaminated with TEP at 150 °C with alternate stirring and sonication for 30 minutes each. The authors mentioned that the cathode interface layer formed during cycling decelerated the PVDF dissolution, which explained that the challenges to directly recycle scraps and spent batteries are different, the latter being more complicated.<sup>10</sup>

In another study reported by X. Song *et al.*,<sup>93</sup> LFP electrodes were delaminated using different solvents such as DMSO, acetone, DMF, NMP and DMAc. Although the use of NMP, DMAc and DMF has shown promising delamination results, a significant volume of solvents was required to achieve >97% efficiency. For instance, the use of DMAc required a solid-to-liquid ratio of 1 : 20 (2 times more than that for the results of

Table 5 Advantages and disadvantages of different delamination methods applied to LIBs

Delamination method	Advantages	Disadvantages
Thermal	Easy to operate Independent on CAM composition	Hazardous gases production and safety risks Costly entrapment or gas management Can degrade/oxidize the CAM Limited to Al melting temperature Not selective, energy intensive, loss of materials The binder cannot be recovered
Mechanical	Simple to operate Widely used Low temperature operation Independent of CAM composition	Require sizing step and in multiple stages Not selective Energy intensive and noise pollution Potential degradation of the active material The binder is still present Not suitable to direct recycling
Chemical	Selectively dissolves and recovers the binder Possible solvent reuse  Simple Can directly recycle CAM High material purity Low environmental impact Low to mild temperature conditions No exhaust emissions	Reagent consumption Solvent selection is dependent on CAM composition (if direct recycling of CAM is expected) Waste chemical treatment CB is considered as an impurity with the CAM

Bai *et al.*<sup>92</sup>), a key parameter for separation efficiency according to Song *et al.*'s<sup>93</sup> research.

In a more recent work, Hayagan *et al.*<sup>46</sup> introduced a novel approach involving pressurized CO<sub>2</sub> combined with a cosolvent mixture of 3 : 1 TEP : acetone. The delamination was conducted at 120 °C and 100 bar for 15 min, reducing the lowest reagent consumption from 1 : 10 for the above-mentioned methods down to 1 : <1.5 (% w/w) of electrode : TEP in this process. This work presented a new method assisted by pressurized CO<sub>2</sub> that 100% delaminate the CAM and CB, and dissolve PVDF in a short time with a low reagent consumption while preserving the integrity of CAM in all aspects. It also allows the recovery of the Al foil and the PVDF binder effectively. The recovered NMC622 showed similar specific capacity and long-term capacity retention compared to that of the pristine NMC622, validating the efficiency of the method. Besides, this approach does not require the use of stirrer, which is a non-neglectable aspect when it comes to treat a large volume of waste.

To facilitate a comprehensive comparison of the various delamination methods, Table 5 summarizes the advantages and disadvantages inherent in each process concerning the delamination of positive electrodes. For selected methods of delamination such as thermal (97%), mechanical (87–94%), and chemical (99–100%) strategies, Hayagan *et al.*<sup>46</sup> reported that the efficiencies vary.

Once the delamination of the composite from the foil is achieved, the active material can be separated from the electronic additive conductor and binder especially with the chemical delamination technique. However, it still cannot be directly used because in EOL batteries, the active material underwent degradation during battery operation, such as structural disordering, particle cracking, transition metal dissolution, and extended CEI growth at the interface with the

electrolyte.<sup>94</sup> For all Li-ion technologies, one of the highlighted mode of degradation is the loss of lithium caused by parasitic reactions such as SEI formation, irreversible structural modifications such as rock-salt type formation at the layered oxide CAM surface, or Li plating.<sup>94</sup> Therefore, the regeneration of the recovered active material becomes imperative for reuse in new battery applications.

To promote the reuse of the degraded positive electrode material, new recycling methods emerged. These methods aim not to lose all the invested energy and cost during the initial synthesis of these CAM, and thus, not to completely damage their structure during recycling processes. Instead, these new direct recycling methods focus on replenishing what is lacking and regenerating materials to achieve enhanced battery performance.

**3.2.2. Cathode material regeneration and upcycling.** This section shows how production scraps and EOL active materials are regenerated and possibly upcycled for subsequent battery production. This direct recycling approach creates a closed-loop system, simultaneously reducing time, energy, and production costs while minimizing environmental impacts.

When an LIB is assembled, inevitable and irreversible degradations happen either during resting or in operation. Over time, as battery ages, its functionality diminishes. This expected deterioration serves as a driving force for recycling, particularly when the capacity falls below 80% of the initial one. Moreover, the degradation extends beyond just the capacity or the electrochemical properties due to the changes in the physical, morphological, structural, and chemical compositions of the electrode material (Fig. 7). Whatever the aging conditions, the CAM always gradually becomes increasingly lithium-deficient as the lithium is consumed through the formation of resistive layers at the surface of both electrodes.<sup>94</sup> In more severe cases, it

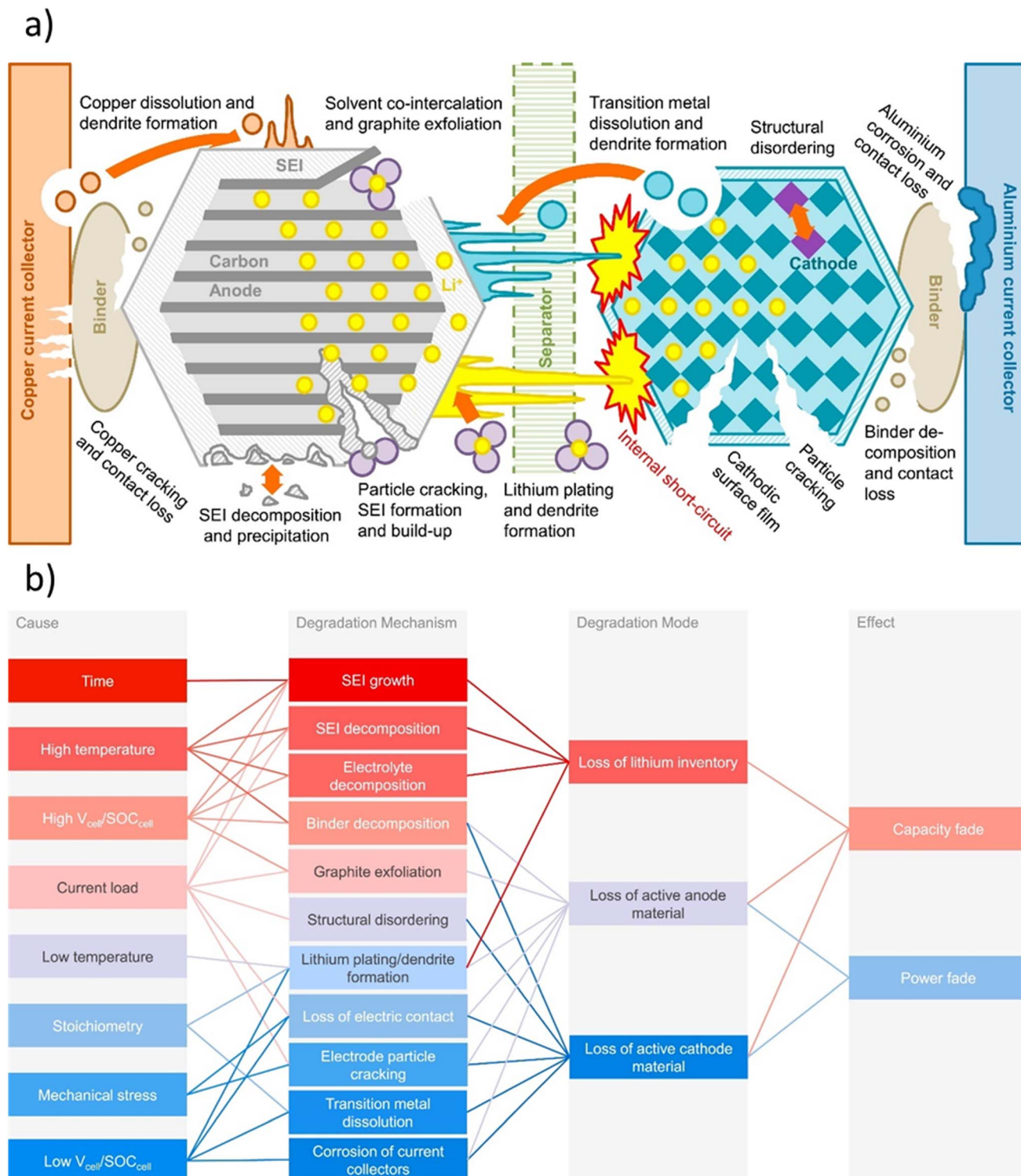


Fig. 7 Schematics of the (a) various possible degradation mechanisms in an LIB cell and the (b) organized cause and effect diagram in LIB cells.<sup>94</sup> Both figures are reproduced with permission from Elsevier.

can entail substantial alterations in composition, structure and morphology. This is due to transition metal dissolution in the electrolyte, transition metal migration within the host structure to often compensate for transition metal dissolution and/or oxygen loss at the interface with the electrolyte, formation of

cracks, *etc.* Hence, after the delamination and separation of the composites (active material, binder, and electronic additive conductor) from the foil, the CAM needs a regeneration step or even upcycling if the technology (nature of active material) is no longer relevant for applications.

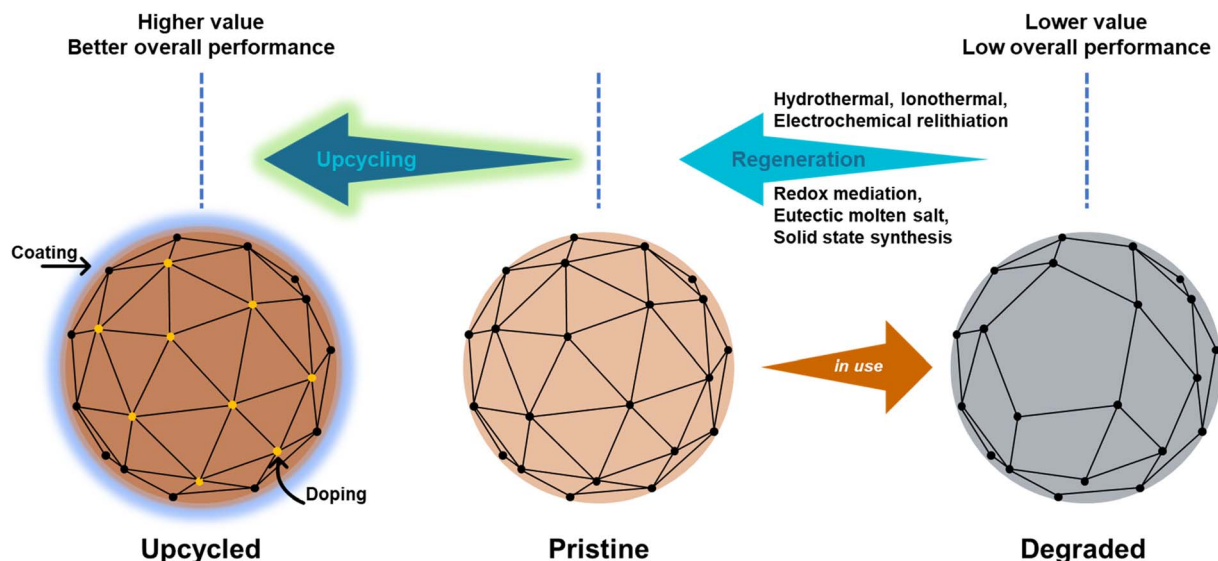


Fig. 8 Different regeneration and upcycling methods for CAM of an LIB.

Table 6 Different parameters employed for the hydrothermal relithiation of various LIB cathodes

Active material	Li loss, %	Li source	Temp., °C	Time, h	Post-treatment	1st discharge capacity, mA h g <sup>-1</sup> (C rate)	Ref.
LCO	20	4 M LiOH or 1 M LiOH + 1.5 M Li <sub>2</sub> SO <sub>4</sub>	220	4	Annealing 800 °C (4 h)	141.9 (2C) 130.3 (5C)	95
LCO + NMC111 1 : 1 (w/w)	20				Annealing 850 °C (4 h) + 5% excess Li source (LiCO <sub>3</sub> )	159 (C/10)	
LMO	13	0.1 M LiOH	180	12	—	111 (C/2)	96
NMC111	22	4 M LiOH	220	4	Annealing 850 °C (4 h) + 5% excess Li source (LiCO <sub>3</sub> )	158 (1C)	97
NMC532						128 (1C)	
NMC111	10	0.1 M LiOH + (3.9 M KOH)	220	2	Annealing 750 °C (4 h) + 5% excess Li source (LiCO <sub>3</sub> /LiOH)	151 (C/3)	98

Direct recycling requires that these aged positive electrode materials are fully repaired and regenerated, from their surface to the bulk. They have to recover their initial composition, structure, morphology, and properties with a minimal input of energy, money, and time, and with the lowest environmental impact. This approach not only closes the loop, but also promotes efficiency and sustainability by reutilizing materials that would otherwise be a waste. By restoring degraded materials, the process contributes to reduced resource consumption and environmental impact, aligning with the principles of circular economy and resource conservation.

Since a lot of different commercial positive electrode materials exist, this following part will present a more generic approach of regeneration conditions that may vary in terms of active material composition. The various approaches, which will be detailed in the following part, are summarized in Fig. 8.

(a) *Hydrothermal relithiation*. Hydrothermal relithiation is a non-destructive approach for regenerating aged and degraded positive electrode materials. The term hydrothermal comes from the high-pressure process using a high ionic strength

aqueous solution containing Li such as lithium hydroxide, as a supply for the Li-deficient powder. The regeneration process usually consists of two steps: (1) the relithiation step whereby chemical composition is regenerated, and (2) thermal post-treatment step commonly called short annealing for microstructural renovation. This strategy aims to ensure comprehensive rejuvenation of CAM and restoration of their characteristics, properties and thus, energy storage performance. Hydrothermal method is by far the cheapest method for regenerating positive electrode materials.<sup>41</sup> It is a simple, green and environmentally friendly method and it can treat EOL electrodes of different lithium contents (see Table 6) without the need for the quantitative analysis of the Li non-stoichiometry. A hydrothermal synthesis route has previously been employed for the production of pristine NMC111 by Wu *et al.*<sup>99</sup> and is now explored to more advanced application in the battery recycling.

A summary of selected papers for the regeneration of different positive electrode materials *via* a hydrothermal process is presented in Table 6. This table highlights the

versatility of hydrothermal regeneration, which is effective across diverse CAM types. A noteworthy observation is that this hydrothermal method is often combined with post-annealing procedures carried out at elevated temperatures, typically close to the conditions employed for the synthesis of the oxide materials. This observation highlights that the hydrothermal process alone is often not efficient enough to recover valuable electrode materials and makes the full regeneration multistep, and thus more energy-consuming.

P. Xu *et al.*<sup>100</sup> used the hydrothermal method followed by post annealing, called targeted healing, of LFP recovered from EOL commercial cells that presented a capacity decay of 50% before disassembly. As compared to some of the results presented in Table 6, often obtained with concentrated Li sources, this study emphasized minimizing LiOH consumption by combining 0.2 M LiOH with a 0.8 M citric acid (CA) solution. To regenerate the degraded LFP, the key points are the filling of Li<sup>+</sup> vacancies while suppressing anti-site defects or preventing their formation. Hence, P. Xu *et al.*<sup>100</sup> used CA to assist the reduction of Fe<sup>3+</sup> within the aged LFP into Fe<sup>2+</sup>, which promotes the insertion of Li<sup>+</sup> to recover stoichiometric LiFePO<sub>4</sub>. The Li composition is regenerated from 0.5 per Fe to 1.0 after only 5 hours of treatment at 80 °C. Regeneration can also be performed at lower temperatures of 70 °C and 60 °C, but with a longer relithiation exposure time of 10 and 17 h, respectively. The aged LFP was characterized by a Li deficiency of 47.1% and by 4.81% Fe/Li anti-site defects, the latter critical parameter being often overlooked in the literature. After the relithiation treatment, the amount of anti-site defects was reduced to 2.2%, even lower than that for the pristine LFP (2.5%). The regenerated LFP with thermal annealing at 600 °C for 2 h delivered a capacity of 159 mA h g<sup>-1</sup> at C/2 with less than 1% capacity loss after 100 cycles, which is similar to pristine LFP with 161 mA h g<sup>-1</sup> at C and negligible decay after 100 cycles. In the following year, P. Xu *et al.*<sup>98</sup> optimized the method with a new solution of 0.1 M LiOH and 3.9 M KOH to further reduce cost and lithium consumption; similar performance was recovered for that regenerated LFP.

Interestingly, H. Gao *et al.*<sup>96</sup> reported a one-step hydrothermal relithiation process for LMO, eliminating the need for an additional annealing step. A reputable capacity of

109 mA h g<sup>-1</sup> at C/2 was obtained for the relithiated LMO compared to 112 mA h g<sup>-1</sup> for its pristine counterpart. However, the main drawback of implementing this one-step process *versus* the one just described is the long exposure time of 12 hours at 180 °C.

Finally, it is also important to emphasize that Ni-rich NMC are sensitive to moisture, making them complicated materials to relithiate especially *via* a hydrothermal approach. Therefore, although promising, this method might not be adapted for all kinds of chemistries. For instance, Sloop *et al.*<sup>101</sup> observed a difficulty in the relithiation of NMC622 due to nickel disproportionation especially at the surface, while Shi *et al.*<sup>97</sup> observed that besides the common spinel phase which are relatively easy to heal, rock salt phase on surface due to Li<sup>+</sup> and the migration of Ni<sup>2+</sup> between layers formed during the degradation or use phase added difficulty on the regeneration. Furthermore, Shi *et al.*<sup>102</sup> suggests that NMC532 requires high O<sub>2</sub> partial pressure to improve the relithiation operation, adding complexity in the regeneration process for this electrode material.

Additionally, the post annealing performed after the hydrothermal relithiation treatment allows cleaning the material's surface from possible hydroxyl groups generated during the hydrothermal process. Thus, the effect of this hydrothermal step on the surface chemistry of each electrode material, and especially on Ni-rich NMC type ones, has to be characterized and understood to successfully develop single hydrothermal step recycling processes.

(b) *Redox Mediation relithiation.* Redox mediation is a low-temperature hydrothermal relithiation process wherein a redox mediator undergoes reversible redox reactions shuttling between two redox states. Unlike hydrothermal relithiation, redox mediation can operate at room temperature and at atmospheric pressure. The mediator acts as a temporary electron carrier, facilitating the transfer of electrons to the electrode material. The process involves a lithiated redox mediator in an electrolyte wherein a Li metal is added to reduce the mediator. The Li metal is removed and the degraded active material is added. The reduced redox mediators by the anode are then oxidized at the cathode surface, transferring Li<sup>+</sup>/e<sup>-</sup> to relithiate the cathode. The electrochemical potential of the redox mediator determines the lithiation voltage; hence, the determination

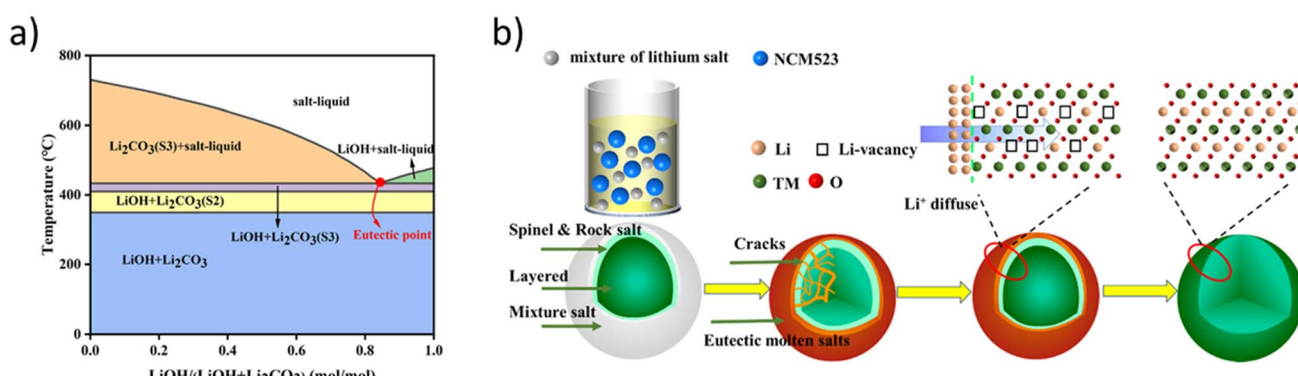


Fig. 9 (a) Phase diagram of a eutectic molten salt system and (b) proposed mechanism in replenishing Li loss.<sup>105</sup> Reproduced with permission from ACS Publications.

Table 7 List of some eutectic molten salts employed in NMC532 healing

Active material	Eutectic molten salts	Temp., °C	Time, h	Post-treatment (time, h)	1st discharge capacity, mA h g <sup>-1</sup> (C rate)	Ref.
NMC532	LiOH : Li <sub>2</sub> CO <sub>3</sub>	440	5	Annealing 850 °C (12 h)	120 (5C)	105
NMC532	3LiNO <sub>3</sub> : 2LiOH	300	4	Annealing 850 °C (4 h) + 5% excess Li <sub>2</sub> CO <sub>3</sub>	124 (5C)	102
NMC532	LiI : LiOH	200	4	Annealing 850 °C (5 h)	150 (C/2)	107

Table 8 Binary eutectic Li salt systems for possible use in eutectic molten salt relithiation technique

Binary Li salt system (A : B)	Eutectic temperature, °C	Mole ratio (A/(A + B))	Binary Li salt system (A : B)	Eutectic temperature, °C	Mole ratio (A/(A + B))
Li <sub>2</sub> CO <sub>3</sub> : LiCl	510	0.64	LiCl : LiOH	273	0.65
Li <sub>2</sub> CO <sub>3</sub> : LiF	613	0.48	LiClO <sub>4</sub> : LiNO <sub>3</sub>	170	0.43
Li <sub>2</sub> CO <sub>3</sub> : Li <sub>2</sub> SO <sub>4</sub>	570	0.60	LiF : Li <sub>2</sub> SO <sub>4</sub>	541	0.61
Li <sub>2</sub> CO <sub>3</sub> : LiOH	430	0.84	LiF : LiI	409	0.83
LiBr : LiF	443	0.24	LiF : LiNO <sub>3</sub>	245	0.95
LiBr : LiI	418	0.64	LiF : LiOH	427	0.80
LiBr : LiNO <sub>3</sub>	223	0.75	LiI : LiOH	177	0.45
LiBr : LiOH	264	0.43	LiNO <sub>2</sub> : LiNO <sub>3</sub>	184	0.42
LiCl : Li <sub>2</sub> SO <sub>4</sub>	470	0.37	LiNO <sub>3</sub> : Li <sub>2</sub> SO <sub>4</sub>	248	0.03
LiCl : LiF	496	0.30	LiNO <sub>3</sub> : LiOH	182	0.38
LiCl : LiI	365	0.64	LiOH : Li <sub>2</sub> SO <sub>4</sub>	399	0.22
LiCl : LiNO <sub>3</sub>	330	0.88			

of Li deficiency of the degraded active material is not required. Mediators can be organic compounds or other non-transition-metal-based organic molecules,<sup>103</sup> acting as reducing agents with low potentials than transition-metal redox couples ideal to fully reduce the positive electrode materials in the presence of a Li salt. Besides, mediators also lower down the activation energy allowing relithiation kinetics to occur at low temperatures, making it a safe process.

In the study of Park *et al.*,<sup>103</sup> a chemically delithiated NMC111 with approximately 10% Li deficiency was used as the sample for demonstrating the capability of this charge shuttling relithiation method. To do so, the authors tested various organic redox mediators such as *p*-benzoquinone, thymoquinone, methyl-*p*-benzoquinone, duroquinone, 1,4-naphthoquinone, 2,5-di-*tert*-butyl-1, 4-benzoquinone and 3,5-di-*tert*-butyl-*o*-benzoquinone (DTBQ), that latter demonstrating the most promising results. Their two-step experiment involved first placing Li metal strips in the DME solution with DTBQ at concentrations ranging from 0.1 to 0.5 M, to prepare lithiated DTBQ solutions. Then, after an overnight stirring, Li metal was removed and the reduced DTBQ molecules were used to perform the relithiation reaction in a batch containing 7.5 mL of lithiated DTBQ solution and 5 g of degraded NMC111. The powder was then recovered, washed with DME and annealed under air at 850 °C for 4 h. The post-annealing is necessary to restore the microstructure of secondary particles because mechanical cracking is a serious material issue in the aged cathode powder. Moreover, such high-temperature treatment allows eliminating the residues of redox mediators still present

in the recovered relithiated active material. After the treatment, the charge capacity of healed positive electrode material *via* redox mediation was at 182.5 mA h g<sup>-1</sup> which is comparable to 184 mA h g<sup>-1</sup> of the pristine state. It was found out that relithiation increases with electrolyte concentration, reducing the reaction time and increasing the throughput.

More recently, Ouaneche *et al.*<sup>104</sup> implemented a greener approach which involves relithiation of spent LFP still casted on the Al collector by simply immersing it in a solution of lithium iodide dissolved in an organic solvent. The authors tested and optimized different reaction parameters such as the temperature, reaction and amount of lithium in different solvents such as acetonitrile, ethanol, cyclohexane, methanol, DMSO and propan-1,2-ol. They took advantages of the redox couple I<sub>2</sub>/I<sup>-</sup> that leads to the spontaneous reduction and relithiation of delithiated LFP in the studied LiI solutions. The regeneration could be carried out at room temperature and on complete LFP cathodes supported on their original current collectors, making the delamination unnecessary. However, they observed some minor corrosion of the Al collector by I<sub>2</sub>.

(c) *Eutectic molten salt solution relithiation.* Eutectic molten salt solution is a mixture of two or more salts, resulting in a lower melting point compared to the individual salts as, for example, LiOH-Li<sub>2</sub>CO<sub>3</sub> (433 °C) against LiOH (462 °C) and Li<sub>2</sub>CO<sub>3</sub> (723 °C)<sup>105</sup> (Fig. 9a). Molten salts are good substitutes to minimize or eliminate the reactivity of NMC systems in aqueous solutions. For instance, this eutectic molten salt approach has been used to synthesize NMC111 by Reddy *et al.*,<sup>106</sup> confirming the structural stability of this active material in such media. The

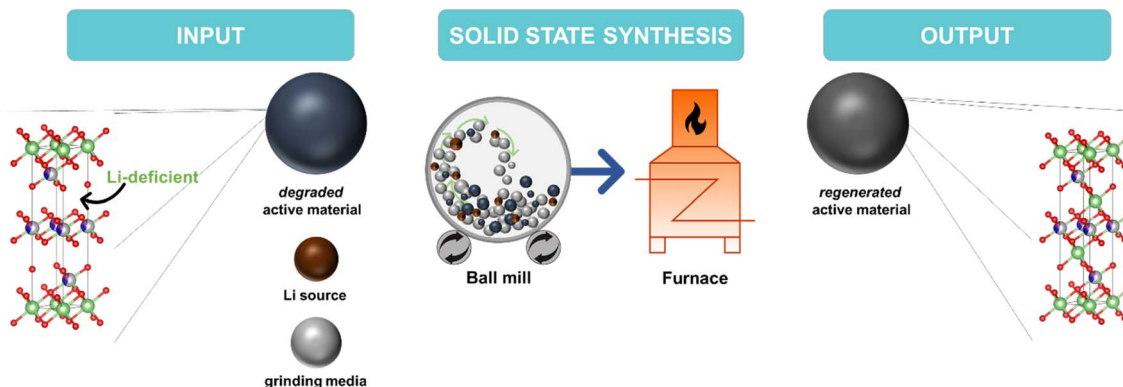


Fig. 10 Two-stage solid-state synthesis schematics: ball milling, followed by a heat treatment, to regenerate the layered oxide cathode active material.

reliothiation mechanism in the Li-based eutectic molten salt medium was proposed by Jiang *et al.*<sup>105</sup> First, the Li salts, in large excess, present at the surface of the Li-deficient active material penetrate within the aggregates through the cracks. Then, due to the Li concentration difference, the Li concentration in salt is much higher than that in the Li-deficient particle, and the  $\text{Li}^+$  ions thus diffuse both at the surface and within the bulk of the active material, filling the Li vacancies and resulting to full regeneration.

The work on the hydrothermal reliothiation of NMC532 presented earlier by Shi *et al.*,<sup>97</sup> was significantly improved by the same team by using an eutectic molten salt mixture in the aim of safer, scalable, low-cost process in regenerating NMC532 even with 40% Li deficiency.<sup>102</sup> With eutectic  $\text{Li}^+$  molten-salt solution, the chemical composition was restored while providing storage capacity, cycling stability, and rate capability back to the pristine levels. The common problem of the NMC system involving the rock salt formation during NMC degradation is also repairable by the molten salt method.

Moreover, according to FactSage,<sup>108</sup> there are a lot of possible binary eutectic Li salt systems that could be explored for the regeneration method, which allows to widely tailor the experimental conditions and adapt the molten salt medium to the specificity of the active materials (temperature stability, reactivity, *etc.*). From Tables 7 and 8, one can easily understand why the temperature can be lowered down by utilizing a different system with the same objective of reliothiation of the same active material.

However, the main drawback of this approach is the use of a large amount of Li salt precursors that would most probably be lost. Moreover, the use of certain eutectic mixtures could lead

to toxic or harmful gas (HF, HCl, *etc.*) released during the reliothiation process that would imply considerable safety measures for a large-scale development. Aside from the listed possible molten salts of two Li sources, a recent publication applies a similar approach by using salt mixtures of  $\text{KCl}$  and  $\text{LiNO}_3$  combined with  $\text{CaO}$  for the regeneration of  $\text{LiCoO}_2$ .<sup>109</sup>

(d) *Ionothermal reliothiation.* Among all the studied methods for positive electrode regeneration, ionothermal reliothiation is the least explored. Ionothermal reliothiation is an electrode material healing method conducted at a low temperature ( $<200$  °C) with non-conventional molten salts called ionic liquids (ILs). Although ionothermal synthesis is an efficient approach for the synthesis of electrode active materials,<sup>110,111</sup> to the best of author's knowledge, only one communication paper is available on its use for the regeneration of active materials. Ionic liquids such as 1-ethyl-3-methylimidazolium bis(trifluoromethanesulfonyl)-imide ( $[\text{C}_2\text{mim}][\text{NTf}_2]$ ), 1-butyl-3-methylimidazolium bis(trifluoromethanesulfonyl)-imide ( $[\text{C}_4\text{mim}][\text{NTf}_2]$ ) and 1-ethanol-3-methylimidazolium bis(trifluoromethanesulfonyl)-imide ( $[\text{C}_2\text{OHmim}][\text{NTf}_2]$ ) were explored as flux solvents for NMC111 direct recycling.<sup>112</sup> The process involves stirring a mixture of chemically delithiated NMC111 (2.5 mmol),  $\text{LiCl}$  or  $\text{LiBr}$  (2.5 mmol), and ILs (2.5 mL) in a 25 mL vial for 10 min, heating to 150–250 °C for 40 min, and then maintaining this temperature for 6–24 h. The mixture is filtered, washed with acetone and ethanol, and dried at 100 °C for 2 h. Small-scale reactions require no calcination, but larger experiments do. For example, a scale-up with 25.3 g of NMC111 (0.263 mol), 3.4 g of  $\text{LiBr}$  (0.392 mol), and 50 mL of ILs (75.3 g) required additional calcination at 500 °C for 4 h, yielding 24.8 g of powder (98.9% yield). The ICP results showed the Li content of regenerated NMC111 at 1.070 compared to 1.072 for the

Table 9 Examples of solid-state synthesis strategy applied to LIBs (LR-NMC =  $\text{Li}[\text{Li}_{0.44}\text{Ni}_{0.136}\text{Co}_{0.136}\text{Mn}_{0.544}\text{O}_2]$ )

Active material	Li loss, %	Li source	Milling time, h	Heat treatment, °C	1st discharge capacity, $\text{mA h g}^{-1}$ (C rate)	Ref.
LCO	11.5	$\text{LiOH} \cdot \text{H}_2\text{O}$ (+5% excess Li)	Ball milling (3 h) + spray drying	900 °C; 12 h	165 (C/5)	113
LFP	N.I.	$\text{Li}_2\text{CO}_3$	Ball milling (6 h)	700 °C; 3 h	152 (C/5)	114
LR-NMC	N.I.	(3 : 2) $\text{LiNO}_3$ : $\text{LiOH} \cdot \text{H}_2\text{O}$	Hand mix in mortar and pestle (0.5 h)	300 °C; 15 h	305 (C/20)	115

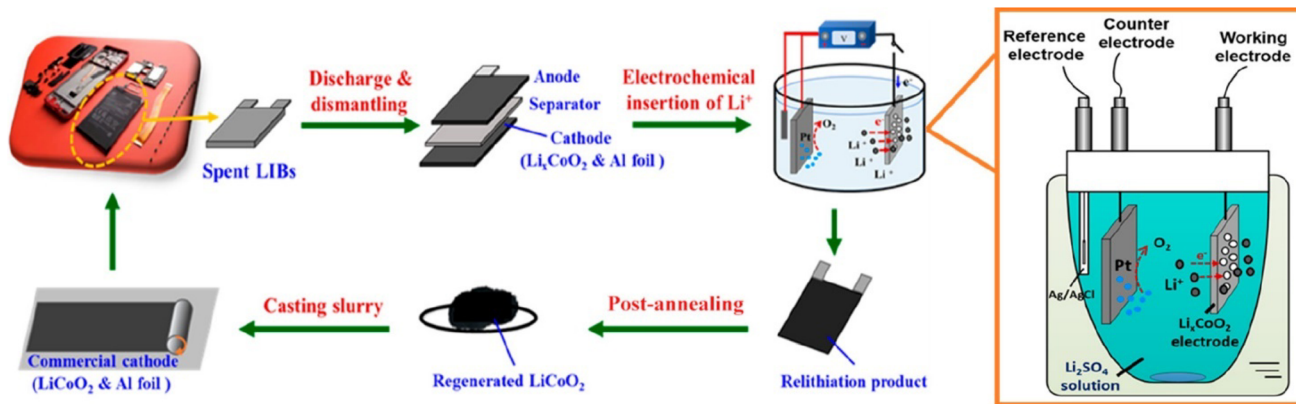


Fig. 11 Electrochemical set-up for relithiating the deficient CAM.<sup>121</sup> Reproduced with permission from ACS Publications.

pristine material, indicating restored chemical composition. X-ray diffraction confirmed relithiation and structure preservation. TGA curves showed identical thermal stability, and no morphological changes were observed. Finally, regenerated NMC111 exhibited an initial capacity of 173.6 mA h g<sup>-1</sup> at C/10, close to the pristine material's 175.3 mA h g<sup>-1</sup>, with similar performance and cycling stability in full cells.

The team identified mechanisms of relithiation exploring the three ILs with LiBr and LiCl salts. For all temperatures of 120 °C, 150 °C and 200 °C, LiBr performs better relithiation than LiCl. Although both halides produce oxidizing gases, the Cl<sup>-</sup>/Cl<sub>2</sub> standard oxidation potential of 1.358 V is higher than Br<sup>-</sup>/Br<sub>2</sub> which is 1.065 V, making LiBr a better Li source for relithiation. Besides, among the three ILs used, namely ([C<sub>2</sub>mim][NTf<sub>2</sub>]), ([C<sub>4</sub>mim][NTf<sub>2</sub>]), and ([C<sub>2</sub>OHmim][NTf<sub>2</sub>]), ([C<sub>2</sub>OHmim][NTf<sub>2</sub>]) was found to be the best solvent because of its hydrophilic hydroxide group which enhances the Li solubility and benefits the relithiation process.

Despite the merits of relithiating at low temperatures compared to eutectic molten salts, the method is not widely explored, possibly due to the cost and availability of ILs compared to traditional solvents and the lack of know-how as it is a very recent method of direct recycling. Thus, a lot has to still be done to better evaluate this approach.

(e) *Solid-state relithiation*. Solid-state relithiation process involves mixing and grinding solid-state precursors to achieve a homogeneous mixture, followed by a high-temperature heat treatment (Fig. 10), usually conducted in a controlled atmosphere to obtain the desired material. This solid-state method is, for instance, widely applied in lithiating carbonate or

hydroxide NMC precursors to obtain the final NMC electrode materials. Hence, it appears as a good option for regenerating lithium-deficient electrode materials with common Li sources such as carbonates, nitrates or hydroxides (Table 9).

Dealing with layered electrode materials, Nie *et al.*<sup>116</sup> and Zhou *et al.*<sup>117</sup> both regenerated spent LCO powders with an almost identical procedure. First, 100 g of the spent powder was mixed with Li<sub>2</sub>CO<sub>3</sub> in a Li/Co ratio of 1.05, calcined in an air atmosphere at 850–950 °C for 12 h, ball milled and sieved with a 400-mesh screen. Before regeneration, the XRD pattern of degraded LCO revealed diffraction peaks at 32.2° and at 36.8° characteristic of the spinel Co<sub>3</sub>O<sub>4</sub> phase, a typical LCO degradation product. These peaks disappeared after the treatments at 800–950 °C, leading to a well crystallized and pure LCO layered phase according to Nie *et al.*<sup>116</sup> The morphology and size of regenerated LCO particles are in good agreement with the expected commercial range of 5–20 µm. The specific surface area of healed LCO is of 0.178 m<sup>2</sup> g<sup>-1</sup> at 900 °C and 0.191 m<sup>2</sup> g<sup>-1</sup> at 950 °C, close to those found for commercial electrode materials (0.2–0.6 m<sup>2</sup> g<sup>-1</sup>). Lastly, the charge capacity of LCO regenerated at 900 °C is 152.4 mA h g<sup>-1</sup>, which corresponds to the one of commercial grade of LCO situated between 140 and 155 mA h g<sup>-1</sup>, validating the regeneration process.

With the same solid-state method, X. Li *et al.*<sup>118</sup> published the direct regeneration of LiFePO<sub>4</sub> materials. In this article, the XRD characterization revealed that degraded LFP contains acetylene black, FePO<sub>4</sub> and P<sub>2</sub>O<sub>5</sub> phases due to delithiation and decomposition in addition to the LFP peaks. These secondary phase peaks started to gradually disappear after treatment of the degraded electrode material with Li<sub>2</sub>CO<sub>3</sub> at 600 and 650 °C

Table 10 Relithiation of LCO using Li<sub>2</sub>SO<sub>4</sub> by different research groups with similar results obtained

Active material (working electrode)	Li solution	Cathodic current, mA cm <sup>-2</sup>	Additional steps	1st discharge capacity, mA h g <sup>-1</sup> (C rate)	Ref.
LCO	1 M Li <sub>2</sub> SO <sub>4</sub>	0.42			
LCO powder	1.5 M Li <sub>2</sub> SO <sub>4</sub>	0.12	Annealing 700 °C (2 h)	136 (C/5)	121
	0.5 M LiOH		Annealing 700 °C (6 h)	130 (C/5)	120
LCO electrode	1.5 M Li <sub>2</sub> SO <sub>4</sub>	0.40		140 (C/10)	

for 1 h in an Ar environment, confirming the regeneration of LFP. The morphology of degraded and regenerated LFP powders are similar, despite the observation of bigger aggregates for the former due to agglomeration brought by the residual binder. The powders treated at 650 °C showed a specific discharge capacity of 140.4 mA h g<sup>-1</sup> and 95.32% capacity retention after 100 cycles.

Although this approach could work for each electrode material chemistry, separately, the downside of this solid-state relithiation is the requirement to quantify the Li deficiency and thus the Li addition necessary for compensation. The homogeneity of mixing, and the impurities from degraded components are not removed and could interfere during the regeneration. Both Nie *et al.*<sup>116</sup> and Liang *et al.*<sup>113</sup> showed that the carbon black and binder have to be removed before the regeneration step. Moreover, this method does not seem to be adapted for a mixture of active materials (e.g. NMC and carbon-coated LFP) due to the different annealing temperatures and atmospheres, not always compatible, required to regenerate the active materials.

(f) *Electrochemical relithiation.* Generally, electrochemical methods are widely used in metal separation and refining such as electrowinning and electrorefining, and recently as a regeneration technique. This method is usually used for electrodeposition and/or electrochemical insertion producing materials with low waste or low reagent consumption.<sup>119–121</sup> Like discharging a battery, the Li deficient electrode material is replenished by applying a voltage to an electrochemical cell allowing Li<sup>+</sup> ions to move from the Li source to the working electrode, which is the Li-deficient electrode material (Fig. 11). One of the main advantages is that the reaction is controlled by electrode potential removing the need to quantify the Li deficiency.

This method was implemented by Ganter *et al.*<sup>119</sup> to regenerate LFP. This latter is stirred for 20 h in an organic electrolyte (1 M LiI in ACN) and Li metal is used both as the counter electrode and lithium source. Although, this method was successful, the Li metal and the electrolyte are both air sensitive making this procedure difficult to set up. To simplify the process, Yang *et al.*<sup>120</sup> introduced an aqueous electrolyte in their work. The team noted that CAM such as LCO, LMO and LFP can be electrochemically relithiated because of their compatible electrochemical windows with that of the electrolyte. Yang's approach involves treating CAM powders with a solution containing 1.5 M Li<sub>2</sub>SO<sub>4</sub> and 0.5 M LiOH. Additionally, they applied the method directly to positive electrode sheets using a solution of 1.5 M Li<sub>2</sub>SO<sub>4</sub>. The procedure is controlled solely by electrode potential. Notably, for the LCO electrode as shown in Table 10, a higher current density was required since the powder is still attached to the Al foil with carbon black.

The electrochemical insertion of Li into the working electrode is both dependent on the concentration of the Li solution and on the applied current density. For example L. Zhang *et al.*<sup>121</sup> demonstrated that, it took 154 min to reach a stable potential with 0.1 M LiSO<sub>4</sub> while 100 min is needed with 1 M LiSO<sub>4</sub>. Additionally, current density increases with the electrons

per unit area, making the insertion faster. In general, comparing this process to the other methods presented, the electrochemical relithiation provides the shortest time to replenish the Li stoichiometry. However, both Yang *et al.*<sup>120</sup> and L. Zhang *et al.*<sup>121</sup> used pristine LiCoO<sub>2</sub> as a lithium reservoir to demonstrate the concept for relithiating lithium-deficient Li<sub>x</sub>CoO<sub>2</sub>. Thus, to be reliable and pertinent, other cheaper and more abundant lithium sources have to be tested/implemented. Additionally, such process could be difficult to upscale from an industrial point of view.

(g) *Upcycling.* It is true that regeneration or healing processes can restore materials to their original composition and structure, but these regenerated materials might no longer meet the flexibility demands of the rapidly advancing battery industry. Therefore, upcycling offers a promising solution to address this limitation. By modifying the chemical composition of battery materials (apart from lithium content), upcycling can yield to new and improved electrode material formulations, effectively repurposing materials that might have lost value due to changes in market demand (see Fig. 8). For instance, transforming NMC111 into NMC622,<sup>41</sup> or applying coatings and dopants to degraded materials during their regeneration can improve their performance and extend their utility. Despite its innovative nature, it is worth noting that upcycling can be more intricate and complex compared to processes focused solely on lithium replenishment.<sup>41</sup> Indeed, for instance, the upcycling process from NMC111 to NMC622 involves structural changes much more complex than a simple topochemical reaction used for relithiation.

Upcycling can be considered as an innovation stemming from previously mentioned processes. For example, as a proof of concept, Qian *et al.*<sup>122</sup> developed a method called molten-salt-based method for direct recycling (MSDR). In their study, Li-deficient NMC532 electrode powder, still containing carbon black and PVDF, was mixed with LiOH, Li<sub>2</sub>SO<sub>4</sub> and Ni<sub>0.83</sub>–Mn<sub>0.09</sub>Co<sub>0.08</sub>(OH)<sub>2</sub>. This mixture was heated first at 900 °C for 5 h and then at 860 °C for 15 h. The resulting product underwent water washing to separate the material from the water-soluble Li salts, dried under air and finally thermally treated at 700 °C for 4 h. From lithium-deficient NMC532, the process led to a fully lithiated NMC-type material containing 66% of Ni called “Ni66-NMC”. The method was further successfully implemented to obtain LiNi<sub>0.8</sub>Mn<sub>0.12</sub>Co<sub>0.08</sub>O<sub>2</sub> from the same degraded NMC532. This time, the upcycling process required a higher amount of Ni source such as using Ni(OH)<sub>2</sub> in addition to LiOH and Li<sub>2</sub>SO<sub>4</sub> that form the molten salt medium and serve as lithium source. This innovative approach of upcycling highlights the potential to extract added value from degraded materials, adapting them to evolving battery material requirements, and contributing to the sustainability and efficiency of battery material management.

A similar approach was introduced by Wang *et al.*<sup>123</sup> who employed a reciprocal ternary molten salt (RTMS) system for electrode material upcycling. This RTMS medium is a mixture of salts that contains multiple anions and cations and enables a low eutectic melting point for the effective flux process at low temperatures. In this study, a chemically delithiated NMC111

was upcycled to fully lithiated NMC622 by using  $\text{Ni}(\text{NO}_3)_2 \cdot 6\text{H}_2\text{O}$  as a nickel source in the  $\text{Li}^+, \text{Na}^+ \parallel \text{Cl}^-, \text{NO}_3^-$  RTMS. Although the method is very promising to obtain NMC622, the authors reported that their attempts to upgrade NMC111 to NMC811 led to an increase in the grain size of the electrode material that finally penalizes its energy storage performance when compared to those of pristine NMC811.

More generally, Gaines *et al.*<sup>41</sup> revealed that NMC systems are difficult to upgrade. This process adheres to specific rules; in the upcycling from NMC111 to NMC622, Li must be initially added to fill the surface vacancies; otherwise, Ni will occupy these vacancies due to its similarity in size to Li, as previously indicated by Shi *et al.*<sup>95</sup> If this substitution occurs, spinels or rocksalt compounds such as  $\text{M}_x\text{O}_4$  ( $2 \leq x \leq 3$ ) or NiO may form depending on the duration and temperature ( $\sim 800^\circ\text{C}$ ) of the process. Hence, the process is efficient only when  $\text{Ni}(\text{OH})_2$  is mixed with relithiated NMC111 and annealed with stoichiometric LiOH, mimicking the original synthesis method for NMC materials. With annealing, it was found out that the initial physical mixture of  $\text{LiNiO}_2$  and NMC111 can equilibrate to a homogeneous NMC622. Additionally, this approach can be used for  $\text{LiMn}_2\text{O}_4$  spinels and NCA. However, this technique is complex because it requires preserving the structure while changing the transition metals stoichiometry, and therefore, there are several challenges such as controlling the coating stoichiometry and its chemical nature, finding the adapted precursor structure type for the upcycling, and blocking the

nucleation at the interface of a phase that would hinder cation diffusion.

Besides upgrading the chemical composition, processes such as coating and doping can be viewed as forms of upcycling, given that they enhance the material's overall performance and increase its market value. This approach also contributes to a higher resource efficiency by extending the material's use, thereby maximizing its value. Additionally, it aids in resource conservation, cost reduction, waste and environmental impact minimization, and energy efficiency.

Wang *et al.*<sup>124</sup> conducted a study on an even more complex hydrothermal regeneration of LCO, combining interface engineering with conventional hydrothermal relithiation treatment. Degraded LCO powders were placed in an autoclave at  $220^\circ\text{C}$  for 4 h with 60 mL of 4 M LiOH solution. Then, the treated sample was recovered, mixed with  $\text{Li}_{1.4}\text{Al}_{0.4}\text{Ti}_{1.6}(\text{PO}_4)_3$  (LATP), ball milled and annealed at temperatures ranging from 700 to  $900^\circ\text{C}$  for 4 h. Then 1–2% of LATP was added to generate mixed-phase substance on the surface of LCO. SEM imaging revealed that nanosized particles formed on the surface of LCO contain a homogeneous distribution of Co, Ti and Al. The powders treated with and without LATP indicated the disappearance of the degradation product,  $\text{Co}_3\text{O}_4$ , and thus a full reconstruction of LCO, and showed an increase in crystallinity. In terms of electrochemical performance, the powders without LATP performed poorly. Conversely, the powders treated with LATP exhibited improved cycle performance, achieving an initial

Table 11 Summary of the advantages and disadvantages of CAM regeneration and upcycling

Regeneration method	Advantages	Disadvantages
Hydrothermal relithiation	High product purity Low to mild temperature operation No Li deficiency determination requirement Self-limiting healing	Material dependent Some cathode requires strict $\text{O}_2$ partial pressure Pressurized vessel requirement
Redox mediation	Requires mediators/reagents Low temperature operation No Li deficiency determination requirement	Complex procedure Mediator stability\and compatibility
Eutectic molten salt solution	Mild temperature operation  Can heal highly Li deficient CAM Two Li sources	Requires two Li-salt's thermodynamic compatibility making a eutectic point
Ionothermal relithiation	Low to mild temperature operation	Non-conventional ionic liquids Expensive
Solid-state synthesis	Simple and easy Can be combined with doping steps	Requires impurity removal Challenge on homogeneity of mixing High energy requirement Energy intensive
Electrochemical relithiation	Room temperature procedure  No Li deficiency determination requirement Easy relithiation monitoring dependent on voltage profile Fast process	High current requirement, requires counter electrode and electrolyte Additives Manned operation
Upcycling	Versatility  Upgrading of value Material adaptability	Li metal is unsafe Requires Li solution Multiple steps requirement (regenerating then coating/doping/upgrading)

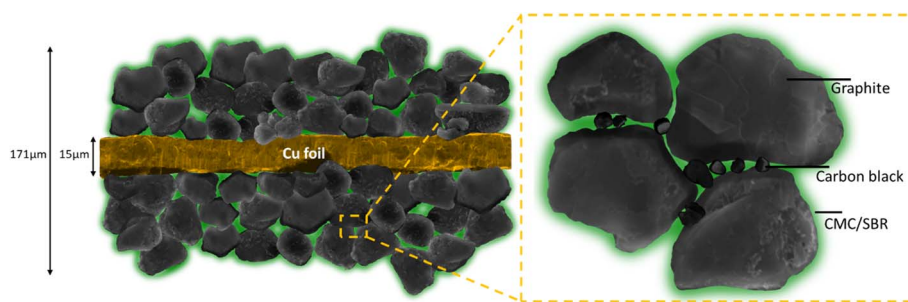


Fig. 12 Negative electrode schematic description highlighting the details of active materials, binders, and carbon black.

discharge capacity of  $150 \text{ mA h g}^{-1}$  that remained at  $147 \text{ mA h g}^{-1}$  after 100 cycles, resulting in 97.5% retention. The morphology of LATP-treated particles showed no visible cracks after 100 cycles compared to non-treated ones and the electrode material maintained a well-defined layered structure, confirming the benefits of the surface engineering. A similar process was conducted by Zhou *et al.*,<sup>117</sup> who not only healed LCO but also doped it with Mg and Ti at Co sites. The electrochemical performance of Mg- and Ti-doped LCO showed an initial discharge capacity of  $177 \text{ mA h g}^{-1}$  and 96% ( $170 \text{ mA h g}^{-1}$ ) retention capacity after 100 cycles, and the performance is much better than that for simply relithiated  $\text{LiCoO}_2$ . The doping of Mg and Ti to LCO provided an improved structural stability and Li diffusion capacity. Similarly, Gao *et al.*,<sup>125</sup> coated LCO with  $\text{Al}_2\text{O}_3$  during the upcycling, which led to electrode materials with a capacity of  $137 \text{ mA h g}^{-1}$  higher than that for the regenerated but not coated LCO ( $133 \text{ mA h g}^{-1}$ ).

Overall, these new and innovative methods are promising despite their complexity especially when viewed in terms of industrial scalability. A summary of the regeneration and upcycling processes is presented in Table 11 according to their advantages and disadvantages. The methods also suggest that different electrode material composition would require different treatments as presented previously. There is not a single solution to all types of materials, leading to complicated challenges to directly recycle or upcycle blended electrode materials. Indeed, some battery manufacturers adopt strategies involving the combination of two or more positive electrode materials, called blended materials, to attain specific properties such as improved power. While this approach enhances overall battery performance and reduces prices, it poses a challenge at the end of the battery's life cycle. The mixing of materials, transitioning from a single chemistry to two or more, introduces complexity in the recycling process, which is a crucial factor to consider for the development of the next-generation of LIBs. Nevertheless, the best relithiation process is the one that is easy to scale-up for production and could be applied to a maximum of different CAM even with mix electrode materials of different levels of Li deficiency.

All the presented relithiation methods target to effectively restore the composition, particularly the Li content, original structure, and electrochemical performance. However, a crucial next step is addressing the limitations inherent in these presented processes, which are primarily designed for known,

clean, and single positive electrode material chemistry. An additional challenge arises when regenerating spent batteries with a different usage history, possibly leading to non-ideal degradation scenarios, with, for instance, inhomogeneities in terms of degradation in the same cell or between different cells. Competitive processes should possess flexibility for accommodating new electrode materials, enabling regeneration for various CAMS such as NMC, LCO, and LFP, even encompassing mixed chemistries found in specific applications. Therefore, achieving a clean feed necessitates enhancing upstream pretreatment processes, such as efficient delamination and separation to remove materials such as PVDF and CB. Moreover, advanced regeneration one-step processes capable of handling mixed materials with differing Li deficiency levels, as well as those containing PVDF and CB, should be developed. The best one that is easy to upscale and has the most cost benefits will be the one in the industry implementation. Therefore, life cycle assessments are needed to evaluate the recycling processes from an environmental, financial, and societal point of view. For instance, the processes using a large amount of solvent and requiring a lot of energy input might not always bring consequent benefits compared to hydrometallurgy approaches.

Finally, while new direct recycling methods show promise, they encounter obstacles such as inadequate battery labeling, logistical challenges of inefficient spent battery collection, and component separation. It can be noticed that the electrode material's chemistry or composition must be known in all presented process, which remains a weakness in direct recycling. However, waste materials, in general, exhibit heterogeneous chemistry, posing significant challenges for implementing direct recycling methods.

### 3.3. Negative electrode delamination, separation, and regeneration

During charging, Li ions intercalate and are stored in the negative electrode and subsequently de-intercalate during discharge to return to the positive electrode. Hence, the negative electrode active material is capable of accommodating Li ions reversibly and efficiently, which is vital for the overall performance of the battery.

Comparing Fig. 6 and 12, the positive electrode is thicker than the negative electrode because the latter has higher capacity. It has to be noted that only crystalline flake graphite can be used as the active material for LIBs, increasing the

Table 12 Advantages and disadvantages of delamination methods applied to the negative electrode

Delamination method	Advantages	Disadvantages
Thermal	Easy to operate	Safety risks (gas evolution) Costly entrapment or gas management Can possibly degrade/oxidize the graphite Possible loss of active material Fluorinated compounds are released in the environment Residual decomposition products, <i>e.g.</i> ashes Requires sizing Not selective Energy intensive Requires Ar or N <sub>2</sub> atmosphere Al melting and breakage Requires classification step especially sizing
Mechanical	Simple to operate Widely used Low temperature operation	Not selective Energy intensive and noise pollution All the components of the composite are still intact Not liberated/separated composites just delaminated Not suitable for direct recycling
Electrochemical	Conservation of morphology	Energy intensive Residual electrolyte could react to media Delithiation of CAM
Chemical	Simple Selectively dissolves and recovers the binder Can directly recycle graphite High material purity Low environmental impact Low to mild temperature conditions No exhaust emissions Conservation of morphology	High reagent consumption Reagent selection is dependent on binder Waste chemical treatment CB is considered as an impurity with the graphite

supply issues. This negative electrode material demands for high performance and long-life, high-purity and highly crystalline structure, which is obtained by pickling and anaerobic high-temperature graphitization at 2800–3300 °C.<sup>126–128</sup> Because of these, natural graphite is a critical raw material in Europe since 2011 and in Japan and the USA.<sup>9,129,130</sup> An effective strategy for graphite is substituting natural graphite with synthetic graphite, which ensures higher purity; hence, the latter is also in high demand. Compared to the extensive positive electrode material family, the graphite constitutes the majority of the used negative electrode materials and demonstrates compatibility with all positive electrode chemistries.

Despite being more stable than the positive electrode materials, graphite also undergoes degradation during its assembly and use (Fig. 7). At EOL, graphite contains a significant concentration of Li and is thus partially reduced, and it is contaminated by electrolyte degradation products (uncontrolled SEI thickness and Li dendrites), binders, and transition metals from the cathode or other additives which complicate the recovery of the active material. Moreover, Li intercalation in graphite intrinsically implies 13% volume expansion,<sup>131</sup> which after long range cycling and successive intercalation and de-intercalation of Li, induces irreversible modifications with a mechanical interlayer spacing and a higher pore size distribution<sup>132</sup> (Fig. 7).

Because of these degradations, there have been many methods that have been tested for graphite recovery. However, the target is to successfully remove Li and other impurities as they might cause short circuit or other battery failure mechanisms. Furthermore, degraded crystallinity and microstructure result in low capacity and low overall battery performance. The direct recycling of the negative electrode also follows the stage process of delamination and regeneration. Below are descriptions of the commonly used direct recycling methods to recover and valorize graphite.

**3.3.1. Different strategies on negative electrode delamination.** Although natural graphite stands as a critical raw material, unlike the positive electrode, there is not a significant body of research available on negative electrode recycling specifically designed to reach a complete LIB direct recycling. Certain methods for delaminating the negative electrode still involve manual scraping, a labor-intensive task that is not readily adaptable for large-scale industrial applications, despite the development of robots for automated delamination. Furthermore, manual scraping leads to challenges for downstream processes even when all the foils are perfectly delaminated because the composites containing graphite, binder(s), and carbon black are still intact and agglomerated along with impurities and other side degradation products. Because it is a mixed material, discriminating these elements for recovery based on their inherent properties poses a considerable

challenge. The following section will present four major delamination approaches currently under development aiming at separating graphite or the electrode composite from the copper current collector (summarized in Table 12).

(a) *Mechanical delamination.* The use of mechanical processing methods in liberating complex electronic wastes is known for years. For minerals, comminution processes such as mechanical crushing are used to liberate ores based on their sizes and mineralogical composition. Van Schaik *et al.*<sup>133</sup> mentioned that the same principle could also be applied to “artificial ores” which are modern consumer products such as LIBs. However, mechanical processes have the main disadvantage of only reducing materials into finer fractions, nothing more. Despite this, there have been many studies implementing mechanical crushing to recycle LIBs.

Wuschke *et al.*<sup>134</sup> studied the comminution of prismatic and cylindrical LIB cells in two crushing stages. They found out that the negative electrode foils can be liberated at a smaller specific size than that of the positive electrode due to difference in adhesive tensile strengths: 1.0 N mm<sup>-2</sup> for positive electrode and 0.4 N mm<sup>-2</sup> for the negative electrode. Finer grinding products were obtained at a higher mechanical energy input; however, they added that an incomplete liberation was observed which reduces the separability of components in downstream processes.

Vanderbruggen *et al.*<sup>88</sup> evaluated three different delamination pretreatment processes aiming to recover active materials from 18650 LIBs. One of the evaluated processes involved mechanical crushing followed by sieving. Majority of the Cu and Al foils were removed in coarser sizes owing to their mechanical properties such as ductility. However, only 5.1 wt% of the black mass was reported to have particles smaller than 63 µm, indicating that while the mechanical process facilitated delamination, it did not effectively liberate the active materials. Indeed, the SEM images revealed the preservation of the binder and thus particle aggregation. The recovered black mass at the finest fraction underwent flotation but the recovery rates were low, around 60% for graphite and the same for lithium metal oxides. Furthermore, mechanical methods such as crushing also have the potential to cause cracks and damages to particles, which induced mechanical stress making difficult the selectivity with regard to specific components. This method has solely the advantage of size reduction, while the delamination efficiency is generally low and separation of active materials from the binder is not achievable. Despite delamination, the composite aggregation persists due to the binder's presence.

(b) *Thermal delamination.* Mechanical processes have proven to be inadequate in liberating graphite effectively due to the persistent presence of the binder. Consequently, the utilization of other processes such as the thermal ones becomes imperative to address this issue. In practice, the use of thermal treatment of negative electrode offers more flexibility than the positive electrode, thanks to the distinct melting points of the current collectors. Specifically, the Cu foil melts at 1085 °C while the Al foil melts at 660 °C. Therefore, there exists a significant gap between the melting points of Cu foil and the binder at the negative electrode especially when treating a black mass.

Therefore, this strategy is better suited to manually separated electrodes. This difference simplifies the process without altering the Cu foil and the active materials as much as possible.<sup>39,134</sup> However, it is crucial to note that O<sub>2</sub> or an air atmosphere cannot be employed in thermal treatments, as they can lead to consumption of graphite.

The team of Vanderbruggen *et al.*<sup>88</sup> exploited vacuum pyrolysis followed by comminution. The aim of this thermal treatment was to decompose the binder at temperatures ranging from 500 to 650 °C. Intact 18650 batteries underwent this method, leading to the partial decomposition of the binder. While this process liberated the negative active material better than mechanical processes, it presented the drawback of Al foil melting.<sup>135</sup> Additionally, possible corrosion due to the generation of HF from electrolyte was noted. After the delamination, they implemented flotation and the recovery of a good grade graphite in the overflow of thermally treated batteries was above 95%, suggesting that this thermal pretreatment process offers a competitive advantage for graphite separation compared to mechanical methods.

Rothermel *et al.*<sup>76</sup> reported a different approach that involves battery shredding followed by electrolyte removal using liquid and scCO<sub>2</sub>. Subsequently, they implemented a process involving magnetic separation for casing recovery, classifiers for separators, thermal treatment at 400–600 °C to decompose the binder, and air-jet sieving to separate the active materials from the foil. Detachment of graphite active material from the foils was observed. However, Raman analyses revealed that implementation of scCO<sub>2</sub> negatively affected the crystallinity of graphite. Indeed, the crystallite size was reduced from 1086 nm down to 635 nm using liquid CO<sub>2</sub> at 60 bar and reduced further down to 279 nm with scCO<sub>2</sub> at 120 bar, revealing the unfavorable effect of pressurized CO<sub>2</sub> on the crystallinity of graphite. However, the team also claimed that this alteration could be due to the state-of-health (SOH) of the cell. Although the recycled graphite showed acceptable cycling stability, a much lower coulombic efficiency was observed in the first cycle, ranging from 79 to 83% for scCO<sub>2</sub> and liquid CO<sub>2</sub>, and attributed to contamination with elements from the positive electrode material. Significant amounts of Li and P were also found in the graphite particles, suggesting that the process was not able to dissolve the SEI and the residual Li salts. This means that CO<sub>2</sub> should be preferentially liquid when extracting the electrolyte as it affects less negatively the anode material.

Similar treatments were implemented by Yang *et al.*,<sup>132</sup> with graphite delamination from Cu foils at 400 °C in an argon atmosphere for 1 h. After separation from the foils, the negative composite material, containing graphite, was further treated at 500 °C for 1 h in an air atmosphere to oxidize the copper impurities and further leach them using a HCl solution. The regenerated graphite was electrochemically characterized using coin cells with Li metal as the counter electrode, with rather high loading (90 wt%) in the potential window of 0.005–2 V at 25 °C. The initial specific capacities were 591 mA h g<sup>-1</sup>, 510 mA h g<sup>-1</sup>, and 335 mA h g<sup>-1</sup> at 37.2 mA g<sup>-1</sup> (C/16), 74.4 mA g<sup>-1</sup> (C/7), and 186 mA g<sup>-1</sup> (C/2), respectively with an excellent columbic efficiency of 100% and a capacity retention

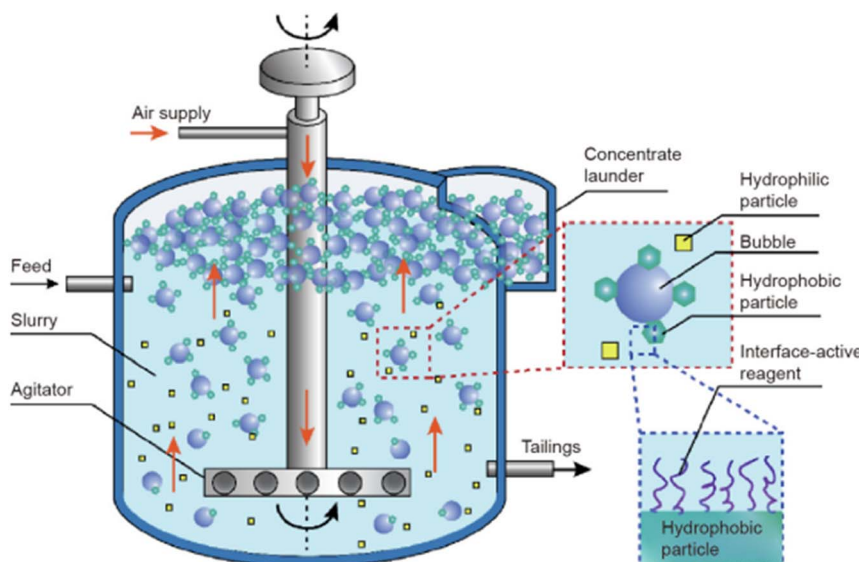


Fig. 13 Schematic of a flotation cell for hydrophobic and hydrophilic material separation.<sup>143</sup> Reproduced with permission from Elsevier.

of 97.9%. This study revealed that, although several steps (leaching and annealing) were conducted to regenerate graphite composition and microstructure, the very high specific capacities, higher than theoretical values, highlighted that some parasitic reactions occurred, and that the recycled graphite does not behave like pristine graphite. Therefore, additional characterizations of the negative electrode material itself and of the electrochemical reaction mechanism are still needed to better understand the reasons behind these phenomena. This also reveals that the recycling process has to be further optimized.

Despite these encouraging results using thermal treatments, Li *et al.*<sup>136</sup> revealed serious environmental pollution because of the generation of gases such as HF, P<sub>2</sub>O<sub>5</sub>, aldehydes and others. Furthermore, when starting from shredded batteries, the method is intrinsically limited to the compatibility with Al melting, showing that prior segregation of the electrodes is required before undergoing thermal processing.

(c) *Electrochemical and/or electro-mechanical delamination.* Cao *et al.*<sup>137</sup> utilized the electrolysis method, which involves applying high voltage to the spent electrode immersed in an aqueous electrolytic solution to peel off the graphite from the current collector. In their setup, the copper foil coated with graphite served as the negative electrode, the spent graphite as the positive electrode and a Na<sub>2</sub>SO<sub>4</sub> solution as the electrolyte. The anode and cathode plates, each weighing 1.5 g, were vertically suspended in 1.5 L Na<sub>2</sub>SO<sub>4</sub> electrolyte solution. The delamination is achieved when the graphite is fully detached from the Cu foil. Plate distance, applied voltage and electrolyte concentration can be optimized to increase the efficiency of the process. An increase in voltage from 10 to 30 V reduces the delamination time of graphite from 200 to 43 min. Similarly, a higher electrolyte concentration as well as a shorter inter-electrode distance tends to increase the motion of ions and increase the current, thereby strengthening the electric field which results in faster and easier separation. Overall, the

procedure was found optimal for 30 V, 2 g L<sup>-1</sup> of Na<sub>2</sub>SO<sub>4</sub> solution and 10 cm distance. However, the recovered graphite (95 wt%) contains traces of fluorine (4–5 wt%) from the binder. It exhibits a first discharge capacity of 427.8 mA h g<sup>-1</sup> at 0.1C, 82% higher than the pristine one. This was due to the higher surface area of the recycled graphite, which provides more sites for Li<sup>+</sup> to intercalate, but it also has a larger SEI film resulting in higher capacity loss. Despite that, a capacity retention of almost 87.4% after the 100th cycle was obtained, revealing competitive performance and efficiency of such approach.

Vanderbruggen's team<sup>88</sup> utilized electrohydraulic fragmentation (EHF), employing successive high voltage pulsations (40 kV) to liberate battery components. Immersing batteries in a water bath facilitated efficient liberation of graphite due to the solubility of the negative electrode binder. The anode binder dissolution and re-hardening after drying led to graphite particle re-aggregation. Lyon *et al.*<sup>138</sup> noted a temperature increase during high voltage pulsations, enhancing binder dissolution. They found that combining mechanical processes with EHF improved the delamination of both the cathode and the anode, with the latter showing a higher efficiency attributed to the anode binder's solubility. Lyon *et al.*<sup>138</sup> also mentioned potential cathode material delithiation, HF formation, and foil comminution at higher energy inputs.

(d) *Chemical delamination.* The soaking of the negative electrode constitutes one of the simplest techniques for delamination. The pivotal factor of this process lies in the dissolution of the binder, choosing the proper solvent medium. For non-water-soluble binders such as PVDF, solvents commonly employed are NMP, DMC, DMF, and DMAc, primarily chosen due to their inherent polarity. For instance, Natarajan *et al.*<sup>139</sup> delaminated graphite from the Cu foil using DMF at 90 °C for 24 h to remove the PVDF. Conversely, DMC was employed by Zuo *et al.*<sup>140</sup>

Water-based delamination of the negative electrode is feasible for water-soluble binders, composed, for instance, of styrene-butadiene rubber (SBR), sodium carboxymethyl cellulose (Na-CMC), or polyacrylic acid (PAA).<sup>141,142</sup> Furthermore, water-based delamination is exclusively viable when the electrode is fully cleaned of any residual electrolyte salt, to prevent any production of HF and damage of battery components and, more critically, any risks to operators involved in the process.

**3.3.2. Separation or purification.** Once the graphite is peeled-off from the current collector, it must be selectively recovered in order to be further re-used or valorized. The following part will present different approaches that are under development for this purpose.

(a) *Flotation.* The flotation method has found application in the separation of materials based on their distinctive physico-chemical properties, primarily focusing on variations in surface wettability (see Fig. 13). In fact, this method separates the graphite from other materials,<sup>88</sup> as, for instance, a distinct dichotomy in wettability exists between graphite and the CAM used as positive electrode materials. Specifically, graphite exhibits hydrophobic characteristics, whereas CAM displays hydrophilic behavior. While this contrast could seemingly facilitate separation, a significant hurdle arises due to the hydrophobic nature of the polymeric binder. As this binder encapsulates both the graphite and positive electrode material, all these components float. Consequently, the pivotal strategy for successful flotation hinges on diminishing or eliminating the presence of the binder material from the surfaces of these active material components.

Different methods such as surface modifications and pyrolysis are employed to remove the binder. One good example was reported by Zhang *et al.*,<sup>144</sup> with a mechanical crushing combined with pyrolysis and then flotation. They found out that the low flotation efficiency is mainly due to residual binders and electrolyte. Batteries from waste mobile phones were discharged with 5 wt% NaCl for 48 h and dried. They were then dismantled manually, and the positive and negative electrodes were crushed with impact crusher for 20 s at a speed of 3000 rad min<sup>-1</sup>. The powder as obtained was then pyrolyzed at 700 °C at a rate of 10 °C min<sup>-1</sup> in a N<sub>2</sub> environment at a flow rate of 20 mL min<sup>-1</sup>. The main findings suggest binder removal due to smoother surfaces of particles and better flotation results. The concentrate grade of graphite was very low at 8.34% with a yield of 80.8%, while they were of 98% and 86.97% for LCO, respectively.

Furthermore, Yu *et al.*<sup>145</sup> used a combination of grinding and flotation. The spent batteries were initially discharged in a solution containing 5 wt% NaCl for 48 h and dried for 1 day. Following manual dismantling, both the positive and negative electrodes were crushed into a mixed fine powder passing through a 0.074 mm sieve. The resulting powder underwent grinding with steel balls for different durations, and the product underwent a two-stage reverse flotation. Methyl isobutyl carbinol (MIBC) was used as a collector during the first stage to recover graphite, and *n*-dodecane as a frother during the second stage to separate LCO from non-liberated LCO. Under the optimum grinding condition of 5 minutes, a graphite

content of 82.57% was achieved with a recovery of 73.6%, and a content of 97.19% with a recovery of 49.3% was achieved for LCO.

The flotation step is mainly referring to increasing the concentration of graphite, wherein the CAM is only separated. However, impurities and other degradation products remain on its surface and in the structure. The purity grade of the recovered graphite is thus not satisfying enough for a second life, encouraging further research to optimize the process.

(b) *Separation and direct re-use.* Sabisch *et al.*<sup>146</sup> adopted a direct reuse approach for the pre-lithiated negative electrode material extracted from spent LIBs. The retrieved active material was subjected to thorough washing processes involving DMC and NMP. DMC was employed to effectively remove any residual electrolyte, especially salt, while NMP was used to strip away the binder. Importantly, the degree of pre-existing lithiation in the active material prior to battery disassembly, the negative electrode composition, and the associated degradation profile were unknown (or not disclosed) in their study.

To evaluate the level of lithiation of the recycled graphite, the initial voltage of assembled cells was measured *versus* Li metal, and in comparison, with pristine graphite. As expected, the latter exhibited an initial voltage of 3.09 V, whereas the recycled graphite displayed an initial voltage of 1.2 V, indicating clear evidence of pre-lithiation. However, the magnitude of this pre-lithiation was determined to be less than 1% of the total capacity, a level insufficient to significantly impact the overall capacity of the recycled graphite material.

Consequently, the graphite containing Li and impurities, along with CB, underwent the addition of PVDF solely, for the purpose of conducting electrochemical tests. The key findings indicated that both the pristine graphite and the recycled lithiated graphite displayed comparable cycling stability. Notably, the recycled graphite exhibited a reduced first-cycle capacity loss, attributed to the beneficial influence of pre-lithiation in facilitating the formation of SEI layer. However, it is identified that the SEI layer was destroyed during the recovery; nevertheless, further characterizations are required to determine the extent of the SEI destruction (distribution and composition) and the nature of the recycled-graphite surface.

A primary drawback associated with this process is the sensitivity of the lithiated graphite to oxygen. Consequently, an inert atmosphere becomes requisite during the various stages of the process. Furthermore, a meticulous manual separation of all battery components during the battery disassembling would be required to preserve the integrity of the intercalated graphite and avoid damaging the SEI layer.

(c) *Hydrometallurgy.* The hydrometallurgy method, commonly employed for recovering valuable transition metals from spent positive electrode materials, is also applicable to negative electrode materials. However, for graphite, it can be considered as a direct recycling approach, in contrast to its application for positive electrode materials. This aqueous treatment approach serves the purpose of eliminating layers present in the negative electrode, such as Li from the electrolyte and the SEI formed during its operational use, alongside other contaminants. It is important to note that positive electrode materials themselves

can be perceived as impurities, particularly in cases where the black mass powder contains both active materials and has undergone size reduction pretreatment. Consequently, this process yields two distinct products: a solution containing dissolved positive electrode materials and the solid graphite retained as a separate component, directly facilitating graphite recycling.

In another study, samples from spent mobile phone batteries were processed by Barbosa *et al.*<sup>147</sup> The graphite was manually separated from the copper foil and then underwent mechanical sieving. The obtained powder was first calcined at 450 °C for 2 h in a nitrogen atmosphere. Subsequently, it was leached with 3 M of HCl at 80 °C for 2 h, washed to neutral pH, filtered and oven dried at 70 °C for 2 h. The recycled graphite did not seem to be negatively affected by the process. The first cycle delivers 390 mA h g<sup>-1</sup>, a higher capacity than expected, but it comes with a huge irreversible loss of 83% efficiency. This “abnormal capacity” was also observed by Yang *et al.*<sup>132</sup> at 0.2C with a value around 500 mA h g<sup>-1</sup>, which was associated with particle and pore size modifications or could be due to impurities of the battery components, structural disorder that affects the SEI and intercalation mechanism, but was not clearly identified.

In a different work, Ma *et al.*<sup>148</sup> treated a black mass containing both the positive and negative electrode components. The black mass was placed in a solution of 5 M sulfate acid with 35% w/w H<sub>2</sub>O<sub>2</sub> at room temperature. Most of the positive electrode material was dissolved in the leaching solution leaving the graphite in the filter cake, which was re-leached a second time under the same conditions to remove further the impurities, before being sintered with an excess of NaOH at 500 °C for 40 min and finally washed and dried. In this last sintering step, recycled graphite reacted with the fusion agent to further remove some remaining impurities, resulting in a better purity than that of graphite recovered without these second leaching and sintering. The sintered recycled graphite showed a capacity of 359.3 mA h g<sup>-1</sup> at 0.2C with a capacity retention of 84.63%

after 100 cycles; however, this performance is degraded *versus* that of pristine commercial graphite showing a lower surface area. Moreover, some graphite was lost at the sintering step, approximately 33 wt%, due to fusion, which strongly lowers the recovery yield.

By hydrometallurgy, dissolving SEI, dendrites, and even the contaminants from the transition metals by acids and bases is simple, however, it has been shown that this strategy could not recover the capacity of pristine graphite because the structure is still not regenerated.

(d) *Regeneration and upcycling.* Unlike positive electrode materials, graphite has persisted as an undefeated negative electrode material, despite recent developments involving silicon doping or mixing silicon with graphite as an active material. Since LIBs entered the market, graphite monopolized the share, owing to its higher capacity than the one of the positive electrode material. Besides, graphite exhibits better stability throughout its lifespan, maintaining its morphology and bulk structure relatively consistently.<sup>94,149,150</sup> The upcycling of graphite, or negative electrode active material, is also undertaken, where graphite is transformed through doping or conversion into highly useful materials such as adsorbent materials.

Gao *et al.*<sup>151</sup> improved the low coulombic efficiency and poor rate performance of regenerated graphite by asphalt coating. The process involved roasting at 600 °C for 2 hours in a N<sub>2</sub> atmosphere to decompose the binder and liberate the graphite. The graphite was then treated with pure H<sub>2</sub>SO<sub>4</sub>, washed with deionized water, cured at 200 °C for 24 hours, and leached with 200 g L<sup>-1</sup> H<sub>2</sub>SO<sub>4</sub> at 90 °C for 4 hours. After neutralizing with water and oven drying at 80 °C for 4 hours, the graphite was roasted again at 1500 °C for 2 hours to remove organics and repair the structure. Finally, the purified graphite was sieved with a 300-mesh sieve and prepared for asphalt coating. For the asphalt coating, a mixture of 0.5 g, pre-sieved at 300-mesh screen, asphalt powder was dissolved in 100 mL of tetrahydrofuran and ultrasonicated for 20 min. The purified graphite was

Table 13 Summarized information of direct recycling companies for LIB applications

Company	LIB components recycled	Latest news on technology	Website
OnTo technology	Positive electrode active materials, electrolyte	Positive electrode healing technology, liquid CO <sub>2</sub> extraction	<a href="https://onto-technology.com/">https://onto-technology.com/</a>
Farasis energy	Positive and negative electrode active materials	Confirmatory tests on electrochemical performance of batteries containing 25% directly recycled positive electrode material, April 2022	<a href="https://www.farasis-energy.com/">https://www.farasis-energy.com/</a>
Duesenfeld	Electrolyte (other components are recovered with traditional recycling methods)	Mechanical thermodynamically electrolyte extraction with no HF production using vacuum distillation/drying technology	<a href="https://www.duesenfeld.com/">https://www.duesenfeld.com/</a>
Ascend elements	Positive and negative electrode active materials	Hydro-to-positive electrode (500 t pilot line in USA and 30 kT per year plant in Georgia, USA) and hydro-to-negative electrode technology	<a href="https://ascendelements.com/">https://ascendelements.com/</a>
Princeton NuEnergy	Positive and negative electrode active materials	Low-temperature Plasma-assisted separation of active materials	<a href="https://pnecycle.com/">https://pnecycle.com/</a>

then added into the solution, which was sonicated for 20 min for dispersion, maintained under stirring at 300 rpm for 3 h and finally evaporated at 80 °C for 12 h. The dried graphite material was ground using a mortar and was again roasted in a vacuum tube furnace at 800 °C for 2 h in an Ar atmosphere. The battery performance was studied as a function of the amount of asphalt coating at the surface of graphite (5, 10, 15, and 20 wt%), which leads to bigger particle size and thus lower specific surface area. The coating is used for repairing surface holes and cracks. The coating amount of 10% gives optimized performance with an initial reversible capacity of 334.5 mA h g<sup>-1</sup> at 0.1C, and a capacity retention of 96.6% after the 50<sup>th</sup> cycle, which exceeded that of pristine graphite of 94.8%, thus confirming the successful upcycling. Nevertheless, this whole process involves many heating, washing and drying steps, which implies the use of significant quantities of acids and solvents and high energy consumption. Thus, LCA analyses should be conducted on this process to estimate its viability for potential upscaling.

Degraded graphite from EOL spent pouch cells was studied by Markey *et al.*<sup>149</sup> After manual disassembly and recovery of the negative electrode by scraping, the collected powder was washed with NMP at 80 °C for 5 h to dissolve the PVDF under stirring. To separate the binder and carbon black, a centrifugation was implemented at 3500 rpm for 5 min; the graphite was washed with distilled water and lastly dried at 80 °C for 12 h. In this study, the regeneration process involves applying a boron-based coating to improve the thermal and electrochemical stability of the recycled graphite. To do so, the recovered graphite was dispersed in a 2 mL solution containing 5 wt% of boric acid, before drying at 80 °C for 12 h and sintered at different temperatures ranging from 750 °C up to 1050 °C for 1 h in a nitrogen atmosphere. After the thermal treatment, the crystallinity of the recovered graphite was enhanced, as revealed by reduced broadening of FWHM, whereas its structure was found similar to that of the pristine. Indeed, the treatment of lithiated graphite by boric acid leads to an acid-leaching and reduction. SEM-EDX shows the presence of O, F, Li, and S besides C, which could be due to residual SEI and electrolyte additives. The boron-based surface coating of graphite allows improving its initial capacity to 330 mA h g<sup>-1</sup> and retained its capacity to 333 mA h g<sup>-1</sup> after 100 cycles, showing a high electrochemical activity and excellent cycling stability.

Another upcycling strategy for spent graphite from EOL LIBs is to convert it into a phosphate adsorbent such as the method presented by Zhang *et al.*<sup>152</sup> At the time of publication, this upcycled material showed the highest adsorbent capability of 588.4 mg g<sup>-1</sup> along with good stability. To obtain this, manually separated anode electrodes from spent 18650 cells were soaked in NMP at 80 °C for 4 h for delamination, filtered off and washed with deionized water before drying in an oven at 80 °C. The obtained powder was soaked in 1.4 M of magnesium nitrate, stirred at 50 °C for 4 h and oven dried. It was then heated at 600 °C for 1 h in flowing N<sub>2</sub>. The final sample was washed with deionized water, dried, and ground. This method salvaged the waste graphite negative electrode into a high adsorbing phosphate material and has the potential to be commercially applied in the industry.

### 3.4. Companies on direct recycling of LIBs

Despite the difficult and complex technology to implement, recently there are significant developments in direct recycling in terms of industrialization and upscaling. To demonstrate the adaptability of the processes designed for direct recycling, Table 13 presents the list of direct recycling facilities.

This demonstration underscores that despite the substantial initial capital expenditure (CAPEX) necessitated by these novel technologies, the direct recycling approach has proven its feasibility and profitability for industrial implementation. This successful commercialization of operations accelerates innovation and creativity, revealing flexibility and opportunities as well as impacts, while making a difference in the field of LIB recycling. This transformative impact not only shapes the landscape of LIB recycling, but also contributes significantly to the broader field, showcasing the potential to effect substantial and positive changes.

## 4. Conclusion and perspectives

This comprehensive review paper has presented an insightful overview of recycling processes employed for LIBs, delving into their inherent strengths, weaknesses, and synergies, with a specific focus on the direct recycling of LIBs and the regeneration of their constituent materials. Indeed, it emphasized that the field is very active, with the development of new direct recycling processes with non-linear approaches challenging conventional practices and invigorating advancements in the LIB recycling field. Historically, elements such as Co and Ni extracted from the positive electrode materials have been the primary targets for recovery due to their high market value, resulting in preferential recycling and consequently lower yields. This highlights a significant strength in the realm of direct recycling – comprehensive recovery of all elements of LIBs, spanning from electrodes to electrolyte components.

Central to the challenge at hand is not solely the enhancement of recycling efficiency and cost reduction, but also the inherent nature of the recycled components. This necessitates a paradigm shift towards the direct reusability of components with minimal resource inputs in terms of time, energy, chemicals, and cost. This vision is attainable through a profound understanding of the intricacies of direct recycling encompassing all facets of LIB components. For the recovered electrode material, its energy storage performance must be evaluated as well as the life cycle assessment of the regeneration process. These two parameters are the keys to evaluate the efficiency and viability of the process.

Despite its complexity, costliness and the prerequisite of presorting, direct recycling holds a unique process by facilitating the maximal recovery of materials and components while preserving their morphology. The recycled materials can be immediately reintroduced into production, mitigating the overall initial synthesis costs. Importantly, while battery technology evolves, the fundamental design remains consistent – laminated and structured as intricate mixtures of various materials. As a result, the methods developed for direct

recycling have broader applicability and efficiency for other battery technologies that share similar designs, and potentially even for materials reliant on layered component lamination. Such an approach could significantly enhance the recycling efficiency and contribute to a more sustainable economic model.

Direct recycling is in no doubt suitable for production scraps, this could also be true for batteries that failed too early wherein the chemistry of active material has not changed. Furthermore, direct recycling will be faced with difficulties with spent batteries especially if these batteries contain mixed positive electrode materials (blends), on top of the technological advancements and changes in positive electrode materials. Therefore, supply chain consideration is a huge deal in taking back materials and fitting them once again in the highly dynamic supply chain of batteries.

Ultimately, the pursuit of processes that uphold the quality of all components emerges as an ideal global standard, setting a benchmark for the industry to aspire to and ensuring a holistic approach to the sustainable recycling of LIBs and beyond. From a circularity perspective, this paper has demonstrated the direct recycling processes for electrolytes, positive and negative electrodes, advocating for a more sustainable approach. Similarly to other recycling processes, the environmental footprint was targeted to be reduced, producing more durable and repairable materials, increasing the material use rate and resource efficiency, while achieving higher recycling rates with the same or higher material value. Because of the substantiated attributes of durability, recyclability, and repairability, LIBs can be acknowledged as energy-efficient products. This can only move forward and further improve the circularity of LIBs.

## Data availability

No primary research results, software or code has been included and no new data were generated or analyzed as part of this review.

## Conflicts of interest

There are no conflicts to declare.

## Acknowledgements

As part of the DESTINY PhD Programme, the authors acknowledge the funding from the European Union's Horizon 2020 research and innovation programme under the Marie Skłodowska-Curie Actions COFUND (Grant Agreement #945357), co-funded by Region Nouvelle Aquitaine (Project Region AAPR2021A-2020-11998810), and from ANR through the STORE-EX Labex project ANR-10-LABX-76-01. This study also received financial support from the French government in the framework of the University of Bordeaux's IdEx "Investments for the Future" program/GPR PPM. We also acknowledge the CNRS.

## References

- 1 J. Frith, *Lithium-ion Batteries: the Incumbent Technology*, Bloomberg NEF, 2019.
- 2 M. Wentker, M. Greenwood and J. Leker, *Energies*, 2019, **12**, 504.
- 3 Electric commercial vehicles: Tax benefits and purchase incentives, 2023, <https://www.acea.auto/fact/electric-commercial-vehicles-tax-benefits-and-purchase-incentives-2023/>, (accessed July 23, 2023).
- 4 C. Pillot, *The Rechargeable Battery Market and Main Trends 2018-2030*, Avicenne Energy, 2019.
- 5 J. Eddy, A. Pfeiffer and J. van de Staaij, *Recharging Economies: the EV Battery Manufacturing Outlook for Europe*, McKinsey & Company, 2019.
- 6 International Energy Agency, *Global EV Outlook 2024 - Moving towards increased affordability*, IEA Publ., 2024, pp. 1-174.
- 7 B. Flipsen, J. Geraedts, A. Reinders, C. Bakker, I. Dafnomilis and A. Gudadhe, *Environmental sizing of smartphone batteries*, 2012 Electronics Goes Green 2012+, Berlin, Germany, 2012, pp. 1-9.
- 8 F. Akbar, *Int. J. Automot. Mech. Eng.*, 2020, **17**, 8310-8325.
- 9 European Commission, Directorate General for Internal Market, Industry, Entrepreneurship and SMEs, *Study on the Critical Raw Materials for the EU 2023: Final Report*, Publications Office, LU, 2023.
- 10 N. Hayagan, I. Gaalich, P. Loubet, L. Croguennec, C. Aymonier, G. Philippot and J. Olchowka, *Batteries Supercaps*, 2024, e202400120.
- 11 M. H. S. M. Haram, J. W. Lee, G. Ramasamy, E. E. Ngu, S. P. Thiagarajah and Y. H. Lee, *Alexandria Eng. J.*, 2021, **60**, 4517-4536.
- 12 J. Zhu, I. Mathews, D. Ren, W. Li, D. Cogswell, B. Xing, T. Sedlatschek, S. N. R. Kantareddy, M. Yi, T. Gao, Y. Xia, Q. Zhou, T. Wierzbicki and M. Z. Bazant, *Cell Rep. Phys. Sci.*, 2021, **2**, 100537.
- 13 N. Horesh, C. Quinn, H. Wang, R. Zane, M. Ferry, S. Tong and J. C. Quinn, *Appl. Energy*, 2021, **295**, 117007.
- 14 D. Kamath, R. Arsenault, H. C. Kim and A. Anctil, *Environ. Sci. Technol.*, 2020, **54**, 6878-6887.
- 15 Y. Tang, Q. Zhang, H. Li, Y. Li and B. Liu, *Energy Procedia*, 2019, **158**, 4304-4310.
- 16 *Regulation of the European Parliament and of the Council*, 2020.
- 17 V. Halleux, *New EU Regulatory Framework for Batteries*, European Parliamentary Research Service, 2021.
- 18 *Regulation (EU) 2023/1542 of the European Parliament and of the Council of 12 July 2023 Concerning Batteries and Waste Batteries, Amending Directive 2008/98/EC and Regulation (EU) 2019/1020 and Repealing Directive 2006/66/EC*, 2023.
- 19 Z. J. Baum, R. E. Bird, X. Yu and J. Ma, *ACS Energy Lett.*, 2022, **7**, 712-719.
- 20 A. Vanderbruggen, E. Gugala, R. Blannin, K. Bachmann, R. Serna-Guerrero and M. Rudolph, *Miner. Eng.*, 2021, **169**, 106924.

21 D. L. Thompson, J. M. Hartley, S. M. Lambert, M. Shiref, G. D. J. Harper, E. Kendrick, P. Anderson, K. S. Ryder, L. Gaines and A. P. Abbott, *Green Chem.*, 2020, **22**, 7585–7603.

22 G. Choe, H. Kim, J. Kwon, W. Jung, K.-Y. Park and Y.-T. Kim, *Nat. Commun.*, 2024, **15**, 1185.

23 D. Werner, U. A. Peuker and T. Mütze, *Metals*, 2020, **10**, 316.

24 T. Zhang, Y. He, L. Ge, R. Fu, X. Zhang and Y. Huang, *J. Power Sources*, 2013, **240**, 766–771.

25 C. Hanisch, T. Loellhoeffel, J. Diekmann, K. J. Markley, W. Haselrieder and A. Kwade, *J. Cleaner Prod.*, 2015, **108**, 301–311.

26 S. Kim, J. Bang, J. Yoo, Y. Shin, J. Bae, J. Jeong, K. Kim, P. Dong and K. Kwon, *J. Cleaner Prod.*, 2021, **294**, 126329.

27 R. Sommerville, P. Zhu, M. A. Rajaeifar, O. Heidrich, V. Goodship and E. Kendrick, *Resour., Conserv. Recycl.*, 2021, **165**, 105219.

28 O. Velázquez-Martínez, J. Valio, A. Santasalo-Aarnio, M. Reuter and R. Serna-Guerrero, *Batteries*, 2019, **5**(4), 68.

29 C. Liu, J. Lin, H. Cao, Y. Zhang and Z. Sun, *J. Cleaner Prod.*, 2019, **228**, 801–813.

30 Y. Yang, E. G. Okonkwo, G. Huang, S. Xu, W. Sun and Y. He, *Energy Storage Mater.*, 2021, **36**, 186–212.

31 T. Georgi-Maschler, B. Friedrich, R. Weyhe, H. Heegn and M. Rutz, *J. Power Sources*, 2012, **207**, 173–182.

32 H. Pinegar and Y. R. Smith, *J. Sustain. Metall.*, 2019, **53**(5), 402–416.

33 H. Heimes, A. Kampker, C. Offermanns, K. Kreisköther, A. Kwade, S. Doose, M. Ahuis, P. Michalowski, S. Michaelis, E. Rahimzei, S. Brückner and K. Rottnick, *Recycling von Lithium-Ionen-Batterien*, 2021.

34 E. Mossali, N. Picone, L. Gentilini, O. Rodríguez, J. M. Pérez and M. Colledani, *J. Environ. Manage.*, 2020, **264**, 110500.

35 S.-H. Joo, S. M. Shin, D. Shin, C. Oh and J.-P. Wang, *Hydrometallurgy*, 2015, **156**, 136–141.

36 K. Davis and G. P. Demopoulos, *RSC Sustainability*, 2023, DOI: [10.1039/D3SU00142C](https://doi.org/10.1039/D3SU00142C).

37 J. Xu, H. R. Thomas, R. W. Francis, K. R. Lum, J. Wang and B. Liang, *J. Power Sources*, 2008, **177**, 512–527.

38 X. Zeng, J. Li and N. Singh, *Crit. Rev. Environ. Sci. Technol.*, 2014, **44**, 1129–1165.

39 L. Sun and K. Qiu, *J. Hazard. Mater.*, 2011, **194**, 378–384.

40 L.-F. Zhou, D. Yang, T. Du, H. Gong and W.-B. Luo, *Front. Chem.*, 2020, **8**, 578044.

41 L. Gaines, Q. Dai, J. T. Vaughey and S. Gillard, *Recycling*, 2021, **6**, 31.

42 G. Harper, R. Sommerville, E. Kendrick, L. Driscoll, P. Slater, R. Stolkin, A. Walton, P. Christensen, O. Heidrich, S. Lambert, A. Abbott, K. Ryder, L. Gaines and P. Anderson, *Nature*, 2019, **575**, 75–86.

43 F. Larouche, F. Tedjar, K. Amouzegar, G. Houlachi, P. Bouchard, G. P. Demopoulos and K. Zaghib, *Materials*, 2020, **13**, 801.

44 L. Gaines, *Sustainable Mater. Technol.*, 2014, **1**, 2–7.

45 J. J. Roy, S. Rarotra, V. Krikstolaityte, K. W. Zhuoran, Y. D.-I. Cindy, X. Y. Tan, M. Carboni, D. Meyer, Q. Yan and M. Srinivasan, *Adv. Mater.*, 2021, 2103346.

46 N. Hayagan, C. Aymonier, L. Crogueennec, C. Faure, J.-B. Ledeuil, M. Morcrette, R. Dedyryvère, J. Olchowka and G. Philippot, *SSRN Electron. J.*, 2024, 1–24.

47 R. Chen, D. Bresser, M. Saraf, P. Gerlach, A. Balducci, S. Kunz, D. Schröder, S. Passerini and J. Chen, *ChemSusChem*, 2020, **13**, 2205–2219.

48 G. Gachot, P. Ribiere, D. Mathiron, S. Grugeon, M. Armand, J.-B. Leriche, S. Pilard and S. Laruelle, *Anal. Chem.*, 2011, **83**, 478–485.

49 N. Susarla and S. Ahmed, *Ind. Eng. Chem. Res.*, 2019, **58**, 3754–3766.

50 M. Ue, in *Lithium-Ion Batteries*, Springer, New York, 2009, vol. 1, p. 41.

51 G. Gachot, S. Grugeon, M. Armand, S. Pilard, P. Guenot, J.-M. Tarascon and S. Laruelle, *J. Power Sources*, 2008, **178**, 409–421.

52 C. Aymonier, G. Philippot, A. Erriguiable and S. Marre, in *Supercritical and Other High-pressure Solvent Systems: For Extraction, Reaction and Material Processing*, The Royal Society of Chemistry, 2018, pp. 304–339.

53 S. Michaelis, E. Rahimzei, S. Brückner and K. Rottnick, in *Recycling of Lithium-Ion Batteries*, PEM of RWTH Aachen And Vdma, Frankfurt am Main, 1st edn, 2021.

54 G. Patry, A. Romagny, S. Martinet and D. Froelich, *Energy Sci. Eng.*, 2015, **3**, 71–82.

55 *The Battery Report 2021*, Volta Foundation and Intercalation, 2022.

56 L. Gireaud, S. Grugeon, S. Pilard, P. Guenot, J.-M. Tarascon and S. Laruelle, *Anal. Chem.*, 2006, **78**, 3688–3698.

57 A. Guéguel, D. Streich, M. He, M. Mendez, F. F. Chesneau, P. Novák and E. J. Berg, *J. Electrochem. Soc.*, 2016, **163**, A1095–A1100.

58 J. Henschel, C. Peschel, S. Klein, F. Horsthemke, M. Winter and S. Nowak, *Angew. Chem., Int. Ed.*, 2020, **59**, 6128–6137.

59 C. Schultz, S. Vedder, B. Streipert, M. Winter and S. Nowak, *RSC Adv.*, 2017, **7**, 27853–27862.

60 C. Schultz, S. Vedder, M. Winter and S. Nowak, *Anal. Chem.*, 2016, **88**, 11160–11168.

61 W. Weber, R. Wagner, B. Streipert, V. Kraft, M. Winter and S. Nowak, *J. Power Sources*, 2016, **306**, 193–199.

62 M. Börner, A. Friesen, M. Grützke, Y. P. Stenzel, G. Brunklaus, J. Haetge, S. Nowak, F. M. Schappacher and M. Winter, *J. Power Sources*, 2017, **342**, 382–392.

63 E. Peled and S. Menkin, *J. Electrochem. Soc.*, 2017, **164**, A1703–A1719.

64 F. Schipper, E. M. Erickson, C. Erk, J.-Y. Shin, F. F. Chesneau and D. Aurbach, *J. Electrochem. Soc.*, 2017, **164**, A6220–A6228.

65 N. P. Lebedeva and L. Boon-Brett, *J. Electrochem. Soc.*, 2016, **163**, A821–A830.

66 T. Träger, B. Friedrich and R. Weyhe, *Chem. Ing. Tech.*, 2015, **87**, 1550–1557.

67 D. M. Werner, T. Mütze and U. A. Peuker, *Metals*, 2022, **12**, 663.

68 G. Zhao, *Reuse and Recycling of Lithium-Ion Power Batteries*, John Wiley & Sons, 1st edn, 2017.

69 H. Yang, G. V. Zhuang and P. N. Ross, *J. Power Sources*, 2006, **161**, 573–579.

70 S. Nowak and M. Winter, *Molecules*, 2017, **22**, 403.

71 S. Sloop and R. Parker, System and method for processing an end-of-life or reduced performance energy storage and/or conversion device using a supercritical fluid, *US Pat.*, US-8067107-B2, 2011.

72 Y. Liu, D. Mu, R. Zheng and C. Dai, *RSC Adv.*, 2014, **4**, 54525–54531.

73 Y. Liu, D. Mu, R. Li, Q. Ma, R. Zheng and C. Dai, *Int. J. Electrochem. Sci.*, 2016, 7594–7604.

74 M. Grützke, V. Kraft, W. Weber, C. Wendt, A. Friesen, S. Klamor, M. Winter and S. Nowak, *J. Supercrit. Fluids*, 2014, **94**, 216–222.

75 M. Grützke, X. Mönnighoff, F. Horsthemke, V. Kraft, M. Winter and S. Nowak, *RSC Adv.*, 2015, **5**, 43209–43217.

76 S. Rothermel, M. Evertz, J. Kasnatscheew, X. Qi, M. Grützke, M. Winter and S. Nowak, *ChemSusChem*, 2016, **9**, 3473–3484.

77 T. Li, X.-Z. Yuan, L. Zhang, D. Song, K. Shi and C. Bock, *Electrochem. Energy Rev.*, 2020, **3**, 43–80.

78 C. K. Lee and K.-I. Rhee, *J. Power Sources*, 2002, **109**, 17–21.

79 J. Lu, K. Minami, S. Takami and T. Adschari, *Chem. Eng. Sci.*, 2013, **85**, 50–54.

80 D. Song, X. Wang, E. Zhou, P. Hou, F. Guo and L. Zhang, *J. Power Sources*, 2013, **232**, 348–352.

81 B. Benallal, C. Roy, H. Pakdel, S. Chabot and M. A. Poirier, *Fuel*, 1995, **74**, 1589–1594.

82 C. Roy, B. Blanchette, B. De Caumia and B. Labrecque, in *Advances in Thermochemical Biomass Conversion*, Springer, Dordrecht, 1993, pp. 11165–11186.

83 L. Sun and K. Qiu, *J. Hazard. Mater.*, 2011, **194**, 378–384.

84 H. Wang, J. Liu, X. Bai, S. Wang, D. Yang, Y. Fu and Y. He, *Waste Manage.*, 2019, **91**, 89–98.

85 J. Liu, X. Bai, J. Hao, H. Wang, T. Zhang, X. Tang, S. Wang and Y. He, *J. Environ. Chem. Eng.*, 2021, **9**, 106017.

86 S. L. Madorsky and S. Straus, *J. Res. Natl. Bur. Stand. Sec. A*, 1959, **63A**, 261.

87 C. Tokoro, S. Lim, K. Teruya, M. Kondo, K. Mochidzuki, T. Namihira and Y. Kikuchi, *Waste Manage.*, 2021, **125**, 58–66.

88 A. Vanderbruggen, N. Hayagan, K. Bachmann, A. Ferreira, D. Werner, D. Horn, U. Peuker, R. Serna-Guerrero and M. Rudolph, *ACS EST Eng.*, 2022, **2**, 2130–2141.

89 J. Öhl, D. Horn, J. Zimmermann, R. Stauber and O. Gutfleisch, *Mater. Sci. Forum*, 2019, **959**, 74–78.

90 O. Buken, K. Mancini and A. Sarkar, *RSC Adv.*, 2021, **11**, 27356–27368.

91 Y. Bai, N. Muralidharan, J. Li, R. Essehli and I. Belharouak, *ChemSusChem*, 2020, **13**, 5664–5670.

92 Y. Bai, R. Essehli, C. J. Jafta, K. M. Livingston and I. Belharouak, *ACS Sustain. Chem. Eng.*, 2021, **9**, 6048–6055.

93 X. Song, T. Hu, C. Liang, H. L. Long, L. Zhou, W. Song, L. You, Z. S. Wu and J. W. Liu, *RSC Adv.*, 2017, **7**, 4783–4790.

94 C. R. Birk, M. R. Roberts, E. McTurk, P. G. Bruce and D. A. Howey, *J. Power Sources*, 2017, **341**, 373–386.

95 Y. Shi, G. Chen and Z. Chen, *Green Chem.*, 2018, **20**, 851–862.

96 H. Gao, Q. Yan, P. Xu, H. Liu, M. Li, P. Liu, J. Luo and Z. Chen, *ACS Appl. Mater. Interfaces*, 2020, **12**, 51546–51554.

97 Y. Shi, G. Chen, F. Liu, X. Yue and Z. Chen, *ACS Energy Lett.*, 2018, **3**, 1683–1692.

98 P. Xu, Z. Yang, X. Yu, J. Holoubek, H. Gao, M. Li, G. Cai, I. Bloom, H. Liu, Y. Chen, K. An, K. Z. Pupek, P. Liu and Z. Chen, *ACS Sustain. Chem. Eng.*, 2021, **9**, 4543–4553.

99 F. Wu, M. Wang, Y. Su, L. Bao and S. Chen, *J. Power Sources*, 2010, **195**, 2362–2367.

100 P. Xu, Q. Dai, H. Gao, H. Liu, M. Zhang, M. Li, Y. Chen, K. An, Y. S. Meng, P. Liu, Y. Li, J. S. Spangenberger, L. Gaines, J. Lu and Z. Chen, *Joule*, 2020, **4**, 2609–2626.

101 S. E. Sloop, L. Crandon, M. Allen, M. M. Lerner, H. Zhang, W. Sirisaksoontorn, L. Gaines, J. Kim and M. Lee, *Sustainable Mater. Technol.*, 2019, **22**, e00113.

102 Y. Shi, M. Zhang, Y. S. Meng and Z. Chen, *Adv. Energy Mater.*, 2019, **9**, 1900454.

103 K. Park, J. Yu, J. Coyle, Q. Dai, S. Frisco, M. Zhou and A. Burrell, *ACS Sustain. Chem. Eng.*, 2021, **9**, 8214–8221.

104 T. Ouaneche, M. County, L. Stievano, L. Monconduit, C. Guéry, M. T. Sougrati and N. Recham, *J. Power Sources*, 2023, **579**, 233248.

105 G. Jiang, Y. Zhang, Q. Meng, Y. Zhang, P. Dong, M. Zhang and X. Yang, *ACS Sustain. Chem. Eng.*, 2020, **8**, 18138–18147.

106 M. V. Reddy, G. V. S. Rao and B. V. R. Chowdari, *J. Power Sources*, 2006, **159**, 263–267.

107 J. Ma, J. Wang, K. Jia, Z. Liang, G. Ji, Z. Zhuang, G. Zhou and H.-M. Cheng, *J. Am. Chem. Soc.*, 2022, **144**, 20306–20314.

108 M. Baben, C. Bale, E. Belisle and Z. Cao, *FTsalt – FACT Salt Phase Diagrams (Version FactSage 8.2)* CRCT-ThermFact Inc. & GTT Technologies, Montreal, Canada 2023.

109 G. Gao, Y. Zhu, S. Di, J. Zhao, C. Liu, S. Wang and L. Li, *Acta Mater.*, 2024, **273**, 119969.

110 N. Recham, J.-N. Chotard, J.-C. Jumas, L. Laffont, M. Armand and J. Tarascon, *Chem. Mater.*, 2010, **22**, 1142–1148.

111 J. Olchowka, L. H. B. Nguyen, E. Petit, P. S. Camacho, C. Masquelier, D. Carlier and L. Croguennec, *Inorg. Chem.*, 2020, **59**, 17282–17290.

112 T. Wang, H. Luo, Y. Bai, J. Li, I. Belharouak and S. Dai, *Adv. Energy Mater.*, 2020, **10**, 2001204.

113 Q. Liang, H. Yue, W. Zhou, Q. Wei, Q. Ru, Y. Huang, H. Lou, F. Chen and X. Hou, *Chem.-Eur. J.*, 2021, **27**, 14225–14233.

114 J. Li, Y. Wang, L. Wang, B. Liu and H. Zhou, *J. Mater. Sci.: Mater. Electron.*, 2019, **30**, 14580–14588.

115 Y. Li, M. J. Zuba, S. Bai, Z. W. Lebens-Higgins, B. Qiu, S. Park, Z. Liu, M. Zhang, L. F. J. Piper and Y. S. Meng, *Energy Storage Mater.*, 2021, **35**, 99–107.

116 H. Nie, L. Xu, D. Song, J. Song, X. Shi, X. Wang, L. Zhang and Z. Yuan, *Green Chem.*, 2015, **17**, 1276–1280.

117 S. Zhou, Z. Fei, Q. Meng, P. Dong, Y. Zhang and M. Zhang, *ACS Appl. Energy Mater.*, 2021, **4**, 12677–12687.

118 X. Li, J. Zhang, D. Song, J. Song and L. Zhang, *J. Power Sources*, 2017, **345**, 78–84.

119 M. J. Ganter, B. J. Landi, C. W. Babbitt, A. Anctil and G. Gaustad, *J. Power Sources*, 2014, **256**, 274–280.

120 T. Yang, Y. Lu, L. Li, D. Ge, H. Yang, W. Leng, H. Zhou, X. Han, N. Schmidt, M. Ellis and Z. Li, *Adv. Sustainable Syst.*, 2020, **4**, 1900088.

121 L. Zhang, Z. Xu and Z. He, *ACS Sustain. Chem. Eng.*, 2020, **8**, 11596–11605.

122 G. Qian, Z. Li, Y. Wang, X. Xie, Y. He, J. Li, Y. Zhu, S. Xie, Z. Cheng, H. Che, Y. Shen, L. Chen, X. Huang, P. Pianetta, Z.-F. Ma, Y. Liu and L. Li, *Cell Rep. Phys. Sci.*, 2022, **3**, 100741.

123 T. Wang, H. Luo, J. Fan, B. P. Thapaliya, Y. Bai, I. Belharouak and S. Dai, *iScience*, 2022, **25**, 103801.

124 Y. Wang, H. Yu, Y. Liu, Y. Wang, Z. Chen, D. Tang, W. Li and J. Li, *Electrochim. Acta*, 2022, **407**, 139863.

125 Y. Gao, Y. Li, J. Li, H. Xie and Y. Chen, *J. Alloys Compd.*, 2020, **845**, 156234.

126 M. Shi, C. Song, Z. Tai, K. Zou, Y. Duan, X. Dai, J. Sun, Y. Chen and Y. Liu, *Fuel*, 2021, **292**, 120250.

127 D. Surovtseva, E. Crossin, R. Pell and L. Stamford, *J. Ind. Ecol.*, 2022, **26**, 964–979.

128 B. Xing, C. Zhang, Y. Cao, G. Huang, Q. Liu, C. Zhang, Z. Chen, G. Yi, L. Chen and J. Yu, *Fuel Process. Technol.*, 2018, **172**, 162–171.

129 G. Blengini, C. Latunusa, U. Eynard and M. Unguru, *Study on the EU's List of Critical Raw Materials – Final Report (2020)*, European Commission, 2020.

130 European Comission, *Critical Raw Materials for Strategic Technologies and Sectors in the EU-A Foresight Study*, 2020.

131 S. Schweidler, L. de Biasi, A. Schiele, P. Hartmann, T. Brezesinski and J. Janek, *J. Phys. Chem. C*, 2018, **122**, 8829–8835.

132 Y. Yang, S. Song, S. Lei, W. Sun, H. Hou, F. Jiang, X. Ji, W. Zhao and Y. Hu, *Waste Manage.*, 2019, **85**, 529–537.

133 A. Van Schaik, M. A. Reuter and K. Heiskanen, *Miner. Eng.*, 2004, **17**, 331–347.

134 L. Wuschke, H.-G. Jäckel, T. Leißner and U. A. Peuker, *Waste Manage.*, 2019, **85**, 317–326.

135 G. Lombardo, *Master's Thesis*, Chalmers University Of Technology, 2019.

136 J. Li, G. Wang and Z. Xu, *Waste Manage.*, 2016, **52**, 221–227.

137 N. Cao, Y. Zhang, L. Chen, W. Chu, Y. Huang, Y. Jia and M. Wang, *J. Power Sources*, 2021, **483**, 229163.

138 T. Lyon, T. Mütze and U. A. Peuker, *Metals*, 2022, **12**, 209.

139 S. Natarajan, D. Shanthana Lakshmi, H. C. Bajaj and D. N. Srivastava, *J. Environ. Chem. Eng.*, 2015, **3**, 2538–2545.

140 X. Zuo, Q. Jiao, X. Zhu, C. Zhang, X. Xiao and J. Nan, *Electrochim. Acta*, 2014, **130**, 156–163.

141 F. Jeschull, D. Brandell, M. Wohlfahrt-Mehrens and M. Memm, *Energy Technol.*, 2017, **5**, 2108–2118.

142 R. Zhang, X. Yang, D. Zhang, H. Qiu, Q. Fu, H. Na, Z. Guo, F. Du, G. Chen and Y. Wei, *J. Power Sources*, 2015, **285**, 227–234.

143 J. Zhang and H. Zeng, *Engineering*, 2021, **7**, 63–83.

144 G. Zhang, Y. He, H. Wang, Y. Feng, W. Xie and X. Zhu, *J. Cleaner Prod.*, 2019, **231**, 1418–1427.

145 J. Yu, Y. He, Z. Ge, H. Li, W. Xie and S. Wang, *Sep. Purif. Technol.*, 2018, **190**, 45–52.

146 J. E. C. Sabisch, A. Anapolsky, G. Liu and A. M. Minor, *Resour., Conserv. Recycl.*, 2018, **129**, 129–134.

147 L. Barbosa, F. Luna-Lama, Y. González Peña and A. Caballero, *ChemSusChem*, 2020, **13**, 838–849.

148 X. Ma, M. Chen, B. Chen, Z. Meng and Y. Wang, *ACS Sustain. Chem. Eng.*, 2019, **7**, 19321–20201.

149 B. Markey, M. Zhang, I. Robb, P. Xu, H. Gao, D. Zhang, J. Holoubek, D. Xia, Y. Zhao, J. Guo, M. Cai, Y. S. Meng and Z. Chen, *J. Electrochem. Soc.*, 2020, **167**, 160511.

150 H. Wang, Y. Huang, C. Huang, X. Wang, K. Wang, H. Chen, S. Liu, Y. Wu, K. Xu and W. Li, *Electrochim. Acta*, 2019, **313**, 423–431.

151 Y. Gao, J. Zhang, Y. Chen and C. Wang, *Surf. Interfaces*, 2021, **24**, 101089.

152 Y. Zhang, X. Guo, F. Wu, Y. Yao, Y. Yuan, X. Bi, X. Luo, R. Shahbazian-Yassar, C. Zhang and K. Amine, *ACS Appl. Mater. Interfaces*, 2016, **8**, 21315–21325.